ForskEL Final Report

Project title	Optimization of Wave Energy Converters' PTO-system Efficiency
ID number	10705
Project period	01.01.2011 - 01.01.2014
Responsible institution	Department of Energy Technology, Aalborg University
Participants	Department of Energy Technology, Aalborg University (AAU) Wave Star A/S (WS) Danfoss Power Solutions (former Sauer-Danfoss ApS) (SD)
Project leader	Henrik C. Pedersen, AAU
Report period	01.01.2011 - 01.01.2014

Preface

This report is the technical documentation for the ForskEL-project no. 10705, carried out in the period 01.01.2011-01.01.2014, and documents the technical contents and findings in the project.

The report is organised in the following parts:

1. Brief summary of project and results. This part may be read independently from the remainder of the report.
2. Technical report, describing the content of the framework, objectives, findings and the technical results of the project. This is an extended summary of the publications found in part four.
3. Outline of project deviations relative to the original plan and reasons here for.
4. List of appended papers.

Dissemination of knowledge within the project group has been in the form of meetings between the involved partners. Public dissemination has primarily been in the form of publishing of papers and presentation of these at conferences. The following papers have been published in relation to the work undertaken in the project:

1. Optimal Discrete PTO Force for Point Absorber Wave Energy Converters in Regular Waves. Hansen, Anders Hedegaard; Pedersen, Henrik C. *In Proceedings of the 10th European Wave and Tidal Energy Conference. 2013*
2. Optimal Number of Pressure Lines in a Discrete hydraulic Force System for the PTO-system in Wave Energy Converters. Hansen, Anders Hedegaard; Hansen, Rico Hjerm; Pedersen, Henrik C. *In Proceedings of the 7th FPNI PhD symposium on Fluid Power. 2012*
3. Optimisation of Working Areas in Discrete Hydraulic Power Take Off-system for Wave Energy Converters. Hansen, Anders Hedegaard; Hansen, Rico Hjerm; Pedersen, Henrik C. *In Proceedings of the fifth Workshop on Digital Fluid Power. 2012*
4. Optimal Configuration of Discrete Fluid Power System Utilised in the PTO for WECs. Anders Hedegaard Hansen; Henrik C. Pedersen. *Submitted to Ocean Engineering - An International Journal of Research and Development*
5. Model Based Feasibility Study on Bidirectional Check Valves in WECs. Anders H Hansen; Henrik C Pedersen; Torben O Andersen. *Submitted to International Journal of Marine Energy*
6. Design of Bidirectional Check Valve for Discrete Fluid Power Force System for Wave Energy Converters. Hansen, Anders Hedegaard; Pedersen, Henrik C.; Andersen, Torben Ole. *In Proceedings of Symposium on Fluid Power & Motion Control, ASME/BATH 2013. 2013*
7. Design of a Multi-Poppet On-Off Valve for Wave Energy Converters. Hansen, Anders Hedegaard; Pedersen, Henrik C.; Andersen, Torben Ole. *In Proceedings of 2013 IEEE International Conference on Mechatronics and Automation. 2013*

8. On/Off Multi-poppet Valve for Switching Manifold in Discrete Fluid Power Force System PTO in Wave Energy Converters. Hansen, Anders Hedegaard; Pedersen, Henrik C.; Andersen, Torben Ole. *Accepted for publication in; International Journal of Mechatronics and Automation.*

9. Design and Control of Full Scale Wave Energy Simulator System. Pedersen, Henrik C.; Hansen, Anders Hedegaard; Hansen, Rico Hjerm; Andersen, Torben Ole; Bech, Michael Møller. *In Proceeding of Fluid power and Motion Control, FPMC2012. 2012*

10. Influence and Utilisation of Pressure Propagation in Pipelines for Secondary Controlled Discrete Displacement Cylinders. Hansen, Rico Hjerm; Hansen, Anders Hedegaard; Andersen, Torben Ole. *Applied Mechanics and Materials, Vol. 233, 29.11.2012, s. 72-75.*

11. Simulation of Utilisation of Pressure Propagation for Increased Efficiency of Secondary Controlled Discrete Displacement Cylinders. Hansen, Rico Hjerm; Hansen, Anders Hedegaard; Andersen, Torben Ole. *Applied Mechanics and Materials, Vol. 233, 29.11.2012, s. 3-6.*

Contents

Chapter 1

Introduction and Project Background

Wave energy has long been considered one of the renewable energy sources, which may aid in solving the worlds energy problems. According to the World Energy Council **[REF!]**, wave energy may in the near future constitute an economically feasible source of 1-5% of the worlds energy demand, corresponding to an energy harvesting of 140-700 TWh/year and in time it is expected that 8.000-80.000 TWh/year may be harvested when wave energy technology advances.

Wave Energy Converters (WECs) are devices designed to convert the energy in ocean waves into a useful form, nowadays typically electricity. As technology, wave energy still lacks a commercial breakthrough. Several WEC concepts have been, and are still being, proposed, and lots have reached the proof-of-concept state showing the ability to extract energy from ocean waves. Yet only very few e.g. the Pelamis Wave Power is known to have a pre-commercial machine [21], which were deployed in a small Portuguese wave farm. The deployment though showed some issues to be bridged to succeed, e.g. storm survivability. Similar one of the key obstacles for the successful deployment of wave energy is the Power Take-Off (PTO)-system, which is also where many of the concepts now having reached proof-of-concept have stranded, as the efficiency of the power take-off systems used are simply much too low to ever have wave energy becoming a economically feasible solution. It is therefore evident to improve the efficiency of the power take-off system, which has also been the focus of the current project.

Wave energy converter concepts are typically classified by the method used to extract energy of the waves, and may be categorised as:

- Overtopping devices: water is lead into a reservoir as waves role onto or into the device. From the reservoir the water is lead back to the ocean through a water turbine, which again drives a generator. The main PTO-system is here the water turbine and the generator. Among other the Wave Plane (by Wave Plane A/S) and the Wave Dragon (by Wave Dragon ApS) are based on this principle.
- Oscillating water column devices: these devices works by using an entrapped water column to create a bidirectional air flow driving an air turbine powering an electrical generator. Devices based on this principle include the Pico power plant and the Mighty Whale (by the Japan Marine Science & Technology Center).
- Attenuators: these contains two or more floating bodies, which are mechanically hinged in a pivot point. Between the bodies are also connected the actuators, which extract the energy from the waves

by applying a damping force opposing the relative motion between the bodies. Dependent on the control strategy the opposing force is controlled in relation to the wave height and velocity to optimise the energy output. Typically the PTO-system is hydraulic, although examples of less mature concepts have also been presented with mechanical transmission systems. Machines based on the attenuator concept include the Dexa WEC and Pelamis.

- Point Absorbers: these devices work by extracting energy from relative motion between two bodies, either two floating bodies or a floating body and a stationary body. The relative movement between the two bodies is what drives the PTO-system. The floating bodies are relative small compared to the wave length and the typical attenuator devices, thereby point absorber WECs excels in been unaffected by the direction of the incoming waves, as oppose to the attenuators. Due to the similarity with attenuators, the power take-off system for the two concepts are however very similar, and typically employs a hydraulic transmission system to drive the electric generator. The Power Buoy, by Ocean Power Technologies (OPT) [19] is an example of a floating point absorbers, whereas the Wavestar, by Wave Star A/S, [23], is a fixed multiple point absorber. The Wavestar differ from the former mentioned point absorbers by having a stationary platform, to which several floating bodies are mechanical attached.

Where the first two groups generally employ turbines (water or air) to drive the generator, the latter two groups typically employ hydraulic power take-off systems for the more mature concepts. Common for many of these devices are that they started out with or have considered purely mechanical transmissions and/or direct drive electrical solutions, and have then emerged to hydraulic power take-off solutions, due the much higher force density and better suited characteristics for WECs, as also concluded in **[15]**. The latter dissertation is the result of the Ph.D. project: *Design and Control of the Power Take-Off System for a Wave Energy Converter with Multiple Absorbers*, between Wave Star A/S and Department of Energy Technology at Aalborg University, which was initiated by Wave Star A/S focus on improving the efficiency of the Power Take Off (PTO) system and thereby increasing the power production of each device. The thesis, **[15]**, include a comprehensive comparison of all the different PTO-technologies, from which it is also found that electrical direct drives are infeasible, due to the poor torque-densities, whereas mechanical transmissions have insufficient durability. Similarly it is also summarised that conventional hydraulic systems suffer from poor efficiency at part load, which constitute a major part of the working conditions for a WEC. The focus of the current project has therefore been on investigating a novel PTO-system based on discrete fluid power technology utilising a secondary controlled fluid power system with common pressure lines. The system may be illustrated as shown in Fig. 1.1, where the concept is illustrated with three pressure lines and two-chamber cylinders.

The idea which has been investigated in the current project is to have each cylinder mounted with a switching manifold so that each cylinder chamber may be connected to one of the different system pressure lines.In the above figure, the concept is illustrated in a system with multiple floats (numbered 1-20), and three pressure lines (red, green and blue) and two-chamber cylinders. Simplified speaking each float is driving a cylinder, which is acting as a pumping unit. The concept may be used with multiple pressure lines and multi-chamber cylinders, with different working areas in the different chambers. By connecting the different chambers to the different pressure lines it is possible to control the force in the cylinder in discrete steps, while keeping the system pressures constant. The latter means that the hydraulic motors used to drive the generators and the generators themselves may work in their optimal range, which is crucial for keeping up system efficiency, as the efficiency of the motors drop rapidly outside the optimal region. Similarly the constant system pressures make it possible to fit accumulators in the system, which adds significantly to the power smoothing. The connections between the different cylinder chambers and the different pressure lines are accomplished via

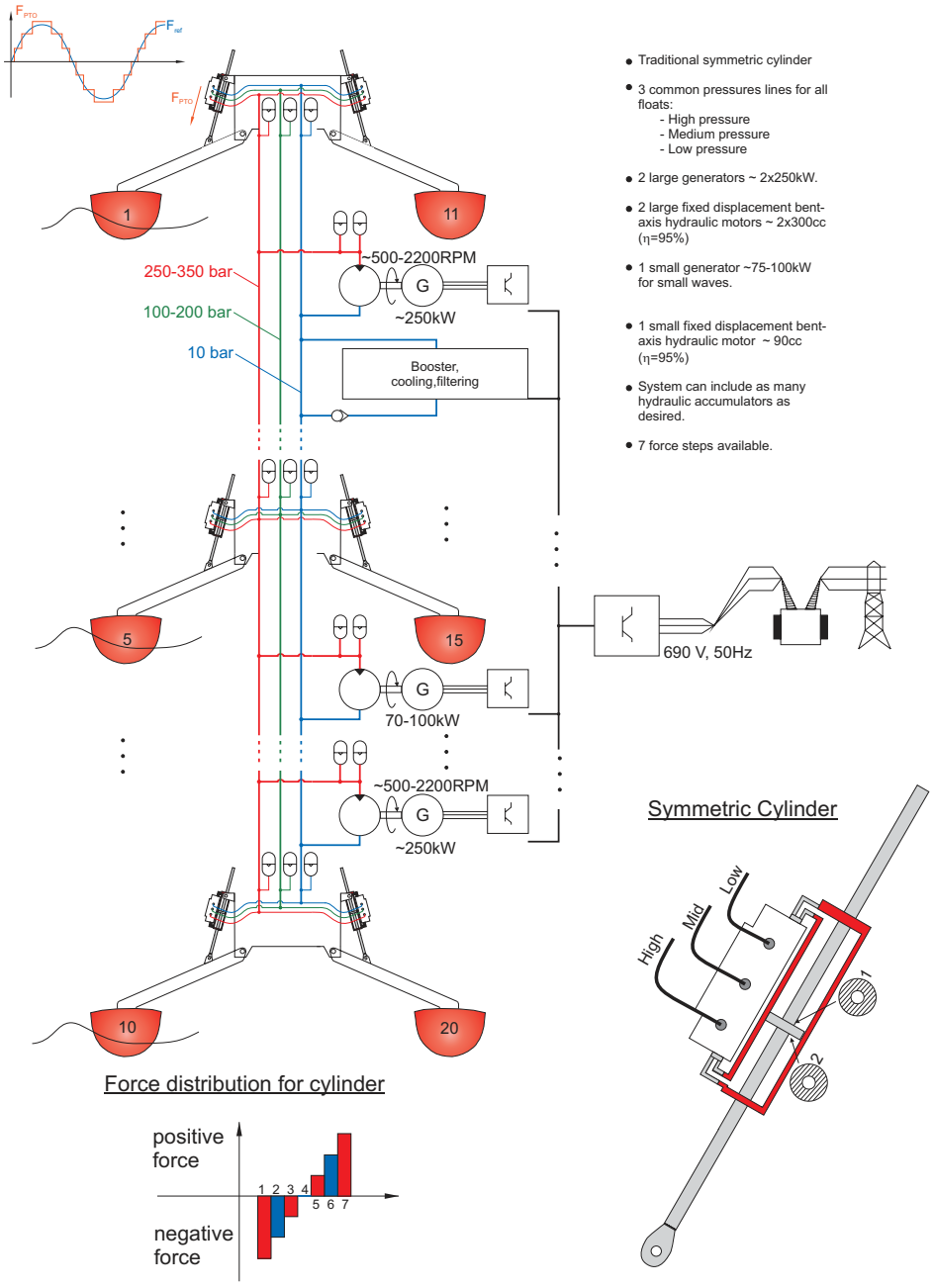

Figure 1.1: System concept, illustrated with three pressure lines and symmetric cylinder.. The "switching manifold" is illustrated by the block on the cylinder with high, mid and low pressure connections.

the switching manifold, which is the key area in this technology. The effect of working with approximately constant system pressures and fairly constant flow ranges to the motors, the latter due to the accumulators, mean that the hydraulic motors used to drive the generators and the generators themselves may work in their optimal range. This is crucial for keeping up system efficiency, as the efficiency of the motors drop rapidly outside the optimal region. The main challenges in this technology is hence the optimisation and control of

the switching manifold to obtain the maximum efficiency.

Based on the above, the following project objective was formulated:

The project objective is to carry out both a theoretical and experimental analysis of the proposed concept to determine the potential improvement in PTO-system efficiency, and create a basis for development of an efficient, reliable and cheap PTO-system. This includes analysis and design of a suited switching manifold and development of control schemes for the system.

1.1 Main Contributions

The project work was originally organised around the following work packages:

- *WP1: Analysis of optimal system pressure levels, accumulation and number of motor-generator systems*
- *WP2: Investigation of requirements to the valves and switching manifold*
- *WP3: Development and optimization of switching manifold*
- *WP4: Development of control strategies*
- *WP5 & WP6: Prototype development of valve configuration (WP5) and testing on test bed in laboratory (WP6)*
- *WP7: Real life implementation and testing on prototype in Hanstholm*

Based on the work packages, the main contributions of this project are the following:

- State-of-the-art analysis concerning digital (discrete force) fluid power solutions. These results are presented in [8], along with a overview of current state-of-the-art concerning fast switching valves and technology.
- A system configuration study of the discrete fluid power force system has been conducted, and a system optimisation method for the discrete fluid power force system based on installation site wave climate has been developed. This includes
  - A generic model of a discrete fluid power force system, usable for optimisation of the PTO-system in WECs has been developed.
  - An investigation of the wave energy extraction for a point absorber WEC in regular waves with a general discrete PTO force system has been made
  - A model based investigation of the potential energy production for various systems configurations has been carried out on how both the sizing of the multi-chamber cylinder and the pressure line distribution affects the power output from the PTO-system of a WEC operating in irregular waves.

  - Development of a method for choosing the system configuration[1] of the Discrete Fluid Power Force system leading to the highest energy production in a given wave climate.

- Development of force switching algorithms (FSAs) to maximise power output, minimise force errors and reduce the loads induced on the mechanical structure due to force switching in the cylinder
- Development of concepts and valves for the switching manifold, hereunder
  - An investigation of feasible valve topologies for switching manifolds utilised in secondary controlled discrete fluid power systems. The investigation was based on a model-based comparison of the potential energy production and system behaviour, when using different valve topologies (on/off-valves and bidirectional check valves).
  - Development of an 800 l/min @ 2 Bar on/off valve main stage, actuated by a Danfoss Power Solution (former Sauer-Danfoss) PVX-pilot valve
  - A conceptual design of both a multi-poppet on/off- and a bidirectional check valve to be used in the switching manifold.
  - Lab testing of the bidirectional check valve concept.
- Installation of first switching manifold on the test-bench and commissioning of the system, hereunder
  - Design, modelling and control of the full scale PTO test-bench. The control refers to the wave system suppressing the correct
  - Installation and commissioning of the valve switching manifold with proportional valves.
  - Preliminary tests have been conducted leading to significant findings for the valve requirements.
- Development and testing of control strategies to maximise power extraction, this includes
  - Investigation of pressure pulsations in the system (PTO-side of test bench), due to valve switching
  - Development of improved controllers for the wave side of the test bench to counteract forces from the valve switching and improve
  - Testing of the force switching algorithm
  - Shaping of the valve opening characteristic (emulated by proportional valves) to minimise pressure pulsations

1.1.1 Deviations from the original project plan

Compared to the original project plan, the project has deviated in relation to WP5, WP6 and WP7, where WP5 have been extended, WP6 have been tested with other than planned valves and WP7 has not been initiated. These deviations are due to 1) prolonged time required for setting up the experimental set-up[2] and delayed commissioning of the test bench, and 2) the manufacturer of the on-off valves not being able to meet

[1] This results in determining the number of pressure lines, the number of cylinders chambers, sizing of the cylinder areas and determining suited pressure levels in the pressure lines.

[2] This is required for testing the switching manifold

the design specifications and requirements for the valves within the time frame of the project. Despite these deviations, the results obtained in the test bench are in so good agreement with the models and the predicted results that the conclusions, which are made on basis of the results of the models and with the test bench, are considered solid. The latter also is based on the performance evaluation of the Wavestar C5 test machine, presented in [16], which supports the utilised models for wave and float simulation used on the test bench set-up.

The deviations to the original project plan are the following:

WP5: Different valve concepts have been considered. This includes on-off valves and a bi-directional valve concept. Different solutions have been investigated:

- A full 800 l/min, 2 Bar on-off valve have been designed and experimentally validated. The results hereof are presented in section **3.** The valve design was a two-stage design, where the pilot stage was based on the Danfoss Power Solution PVX-pilot stage. The valve fulfilled all design requirements wrt. flow, pressure and dynamic requirements. Utilising two pilot valve spools in parallel and the lack of a pilot spool feedback, however complicated the main spool control, if this was to be controlled more intelligently than merely on-off, which was the intention to implement artificial end damping to increase the lifetime of the valve. For this reason the design was put on hold, as discussed in chapter 3 and Danfoss Power Solutions involvement in the project reduced.
- In collaboration with Bucher Hydraulics, a commercial two stage on-off valve has been specified, which was designed specifically for the Wavestar WEC. The design is still in the prototype phase and in is still under test at Bucher Hydraulics.
- Conceptual design and dimensioning of both a multi-poppet on-off valve and a bidirectional check valve have made been made, and the two concepts have been compared with regard to feasibility, energy output and loads imposed on the mechanical structure when switching [E]. The studies show that systems using bidirectional check valves are highly competitive on energy output, but may introduce extra loads on the mechanical structure of the WEC. The functionality of the bi-directional check valve was furthermore experimentally tested and validated.

WP6: The experimental set-up has been modified from initial plans and include the first prototype (referred to as P1) of the switching manifold, which has been based on a special commercially available 2/2-proportional valve. In the present form this valve will not be a realistic alternative for wave energy converters, due to both price and lack of robustness. However, due to the valves high bandwidth and these being proportionally controllable, they are very suited for testing the concept in the test-bench, where it is possible to emulate the behaviour of other valves. This has made it possible to test most of the dynamic aspects related to the presented concept. I.e. testing with the P1 has brought invaluable knowledge for the upcoming prototypes. Significant work has furthermore gone into making the test bench ready for testing the valves, developing control strategies, so the wave side of the system correctly emulates the wave and float behaviour and implementing and testing strategies these on the test bench. However, this work is only sparsely documented in the present report, as this is merely a requirement for being able to properly test the switching manifold.

WP7: Due to the changes in WP5 & WP6, it has not been realistic or desirable to test the switching manifold on the Wavestar WEC. The P1 manifold is not suited for operation on the WEC, and focus has therefore instead been shifted to investigating the loading effects of valve switching and improve the valve characteristics to reduce the force peaks as described above.

1.2 Overview of Results and Report Structure

The results of the project is evaluated in relation to each of the work packages, although several of the results from different WPs are combined in single chapters for easier readability. The primary results of the project have all been published in various conference papers and journal papers (some still awaiting publication), and most of the results are also included in the PhD-dissertation[3], [8], which is also a result of the work in the current project. This report is hence largely based on the extended summary in the PhD-dissertation and is a summary of these main results. Details of the models etc. are not included in the current report, but may be found in [8]. For a further elaboration and more detailed discussion of the results the reader is therefore referred to the corresponding articles[4]. The following papers constitute the background for the report (full information is given in the Bibliography):

Paper A *Optimal Discrete PTO Force for Point Absorber Wave Energy Converters in Regular Waves*. [7]

Paper B *Optimal Number of Pressure Lines in a Discrete hydraulic Force System for the PTO-system in Wave Energy Converters*. [1]

Paper C *Optimisation of Working Areas in Discrete Hydraulic Power Take Off-system for Wave Energy Converters*.[2]

Paper D *Optimal Configuration of Discrete Fluid Power System Utilised in the PTO for WECs*.[3]

Paper E *Model Based Feasibility Study on Bidirectional Check Valves in WECs*.[9]

Paper F *Design of Bidirectional Check Valve for Discrete Fluid Power Force System for Wave Energy Converters*.[5]

Paper G *Design of a Multi-Poppet On-Off Valve for Wave Energy Converters*. [4]

Paper H *On/Off Multi-poppet Valve for Switching Manifold in Discrete Fluid Power Force System PTO in Wave Energy Converters*. [6]

Paper I *Design and Control of Full Scale Wave Energy Simulator System*.[20]

Paper J *Influence and Utilisation of Pressure Propagation in Pipelines for Secondary Controlled Discrete Displacement Cylinders*.[11]

Paper K *Simulation of Utilisation of Pressure Propagation for Increased Efficiency of Secondary Controlled Discrete Displacement Cylinders*.[12]

The following papers are furthermore the result of the collaboration between the current project and the industrial PhD-work by Rico H. Hansen [15]. The results are presented in [15] and constitute some of the background for the valve design specifications and the feasibility of a discrete force PTO-system:

Paper L *Analysis of Discrete Pressure Level Systems for Wave Energy Converters*. [13]

[3]The dissertation is made as an extended summary and a collection of papers.

[4]The articles are not included in the report due to copyright reasons, but a copy of the articles will be uploaded to ForskEL (not for redistribution).

Paper M *Determining required valve performance for discrete control of PTO cylinders for wave energy*.[10]

The papers A-D addresses the problems of the optimal configuration of a discrete force PTO-system, and the results of these findings are summarised in Chapter 2. A fundamental study on configuration of a fluid power force system for wave energy converters is given in chapter 2. The system configuration in terms of choice of number of common pressure lines and the pressure level at which they should be operated is initially investigated and presented in paper B. Secondly the sizing of the multi-chamber cylinder is investigated in paper C. The combination of the studies on configuration of the common pressure lines and multi-chamber cylinder is presented in paper D. Here a framework for choosing the optimal system configuration for a given installation site is also demonstrated.

The configuration of the switching manifold is investigated in terms of valve type and valve design. Hence, a topology investigation of a Bidirectional Check (BC) valve versus an on/off valve is initially conducted. A comparison of energy output, dynamic behaviour and structural loads when using BC- and on/off-valves are given in paper E. The studies show that systems using bidirectional check valves are highly competitive on energy output. However, this comes at the expense of an expected increase in structural loads. A conceptual valve design is given for the bidirectional check and the on/off valves in papers F and G respectively. A multi-poppet topology is utilised for the BC and on/off valve. Only minor difference in actuation area on the main stage and connection in the pilot system separates the two valve designs. A conceptual multi-poppet design is given for both the BC and the on/off valve allowing valve switching faster than 10 ms using a 3/2 way direct electronic actuated pilot valve.

The bidirectional check valve concept was tested in paper F, where the concept was found applicable, however the utilised test set-up did not enable switch time measurement. Furthermore preliminary results from the full scale PTO test-bench are given in this dissertation, however no publication of the results have yet been submitted due to an ongoing commissioning phase.

References to the various articles will be made throughout the report. The remainder of the report is organised as follows.

Chapter 1 This chapter has given a short presentation of the problem at hand, an overview of the main results of the project and an outline of the report.

Chapter 2 Present the findings for the optimal system configuration. Results for the optimal discrete PTO force profile are presented for both a simplified heave motion point absorber, and when considering more complex wave conditions. Results for using the system as PTO element in the Wavestar machine is furthermore presented, which are based on a generic model of the discrete fluid power force systems, which has been used for the brute force optimisation of the system. Included in the chapter are furthermore the developed Force Shifting Algorithms (FSAs), as these are an integrated part of evaluating the optimal system configuration. Finally the chapter ends with a presentation of the method which has been developed for choosing a proper system configuration based on maximal energy output, taking into account the time distribution of sea conditions.

Chapter 3 Summarises the main findings for the different valve concepts considered and the design considerations regarding the switching manifold. First the results related to the design of a standard on-off valve based on the Danfoss Power Solutions PVX-pilot valve are presented. Secondly the results for a model based

feasibility study of using the bidirectional check valves are presented along with a conceptual design for both the bidirectional check valve and an on/off-valve concept both based on a multi-poppet valve principle. It is shown that both concepts are capable of active switching in less than 10 ms. The chapter is concluded with a proposal of utilising both on/off and one directional check valves with on/off valve possibilities in the switching manifold.

Chapter 4 Describes the main results of the work with the test bench and the experimental results obtained. This include a discussion of the control of and work related to implementing and testing the discrete force concept on the test bench. Results are presented, which validates the behaviour of the test bench and results from the valve switching tests conducted on the P1 prototype manifold are presented. It is shown how the valve switching time affects the cylinder chamber pressure and how pressure oscillations are experienced in the transmission lines from manifold to cylinder chambers.

Chapter 5 Overall summary of the main conclusion of the present work.

Appendices This report serves as an addition to the papers published during the project period. These are found in the appendix. The appended papers are given in the original layout, however resized to fit the present paper size.

Chapter 2

Optimal System Configuration

The configuration of the PTO-system for wave energy converters highly affects the system efficiency and the potential energy extraction. The configuration here refers to the number of chambers in the PTO-cylinder, the piston areas associated with each chamber and the force levels in the pressure lines, as seen in Fig. 1.1. This term will be used throughout the report.

The applicable forces, which are a results of the pressure in the different cylinder chambers and the piston areas, directly affects the energy extraction by setting the bounds for the power levels obtainable in a given sea conditions. Hence, the applicable forces may be optimised to maximal the energy extraction. The goal is, however, not to maximise the extracted energy out of the waves, but the power to the grid. The conversion of the extracted energy into output energy is here unaffected by the applicable force, but highly affected by how the forces are generated, and in particular the energy losses associated herewith. The configuration of the discrete fluid power force system is hence a trade-off between yielding good energy extraction ability and yielding high energy conversion efficiency.

For commercial success of wave energy converters the energy output has to be high compared to the installation and maintenance cost, yielding a low cost of energy (Euro/kWh). With cost of energy as main focus, high conversion efficiency and large energy extraction both becomes sub-objectives in the configuration of the PTO system. However, these two sub-objectives may aid the primary objective of having a high energy output of the PTO. Furthermore low system efficiency is often aligned with large wear in system components.

In this chapter the system configuration the results of the analysis of the discrete fluid power force system are presented. Initiating with a discussion of how the number of discrete forces and the size of these affect the energy extraction capability of the wave energy converter. The PTO model has been combined with a model describing a single float of the Wavestar and the float wave interaction. This model has been used to conduct a system configuration optimisation of the discrete fluid power PTO-system. The parameters optimised are the multi-chamber cylinder and the common pressure lines, in terms of the chamber numbers and their size and the pressure levels and number of common pressure lines.

2.1 Results from Simplified Analysis of Energy Extraction with a Discrete PTO Force

To get an idea of how the force levels, switch times of the valves and number of force levels affect the power output of the system, a simplified analysis have been conducted, for a much simplified systems as shown in Fig. 2.1, which also illustrates the different problems associated with design the optimal switching manifold for a WEC. The analysis has been made where the float, shown in part (a) of Fig. 2.1, is subject to a regular wave, which is described by a pure sine motion. Assuming a standard power extraction algorithm for the system, the ideal force, which the PTO-system should exert on the float will therefore also be described by a pure sine signal. However, due to the discrete nature of the considered PTO-system, the system is only capable of producing a fixed number of discrete force levels, which are dependent on the number of pressure lines in the system and the number of chambers in the cylinder. The size of the force is furthermore dependent on the piston areas in the cylinder. For the simple case, where the system is designed with a symmetrical two chamber cylinder and two pressure lines, three different forces may result, as shown in the upper part of part (d) in Fig. 2.1. For a system with three pressure lines the number of force levels however potentially increase to seven different levels or five if pressure lines are equally distributed level wise. The latter is shown in the lower part of Fig. (d). The applied force from the PTO-system may therefore be considered as box contributions, as shown in part (e) of the figure. The questions for the discrete force systems is therefore not only, how many force levels are required and the size of these, but also, when they should be "switched in" to give the best power extraction - in this connection it is important to realise that although the ideal force reference for a continuous system may be sinusoidal, this may not be the case for the discrete force system, as the system cannot track this reference anyhow. For the system to represent the ideal force, the switching times (a_i's and b_i's in the figure) of the valves therefore need to be considered as well.

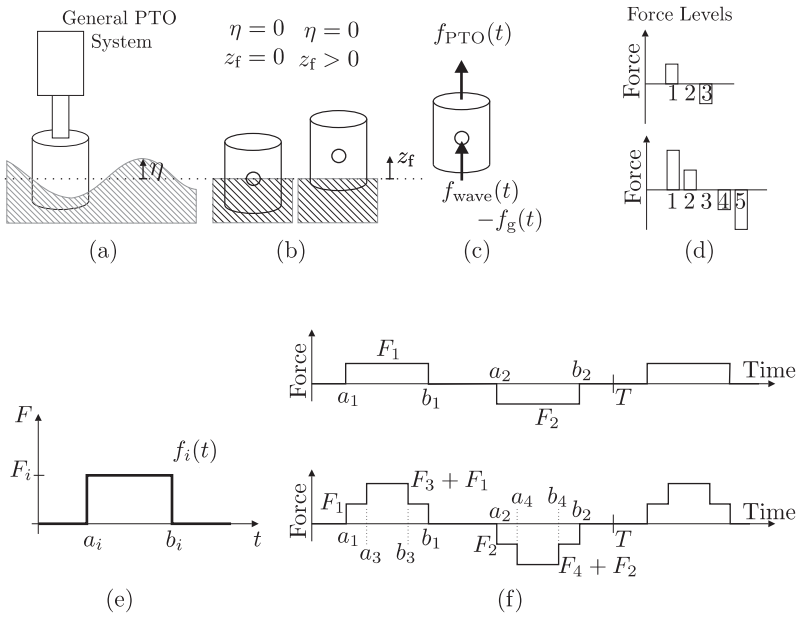

Figure 2.1: Illustration of; the simple float model (a), (b), (c); applicable discrete force levels (d); single box force (e) and the discrete force profile(f).

In this section the results of a the analysis of a simplified system is therefore presented. The results have

here been obtained through an analytical approach to the problem, of which discrete force levels to apply and how many of these are required, is solved for a point absorber operating in monochromatic waves. This has been done by developing a much simplified model for the float movement and the wave-float-interaction. By exploiting linearity of the simplified model an analytical solution of the float movement and the energy extraction is found, for the float working in monochromatic waves under influence of a discrete, but periodic PTO force. As described in the introduction the initial investigation has therefore been made to get an idea of how the system configuration should be for the simple case of a regular wave, and without losses in the PTO-system included, to see how this influence the power extraction of the system. The results and the detailed analysis may be found in paper A, [7]. The results in the following sections, on the other hand, include the fluid power system and hence losses.

2.1.1 Extracted Energy

To get an idea of the results the definition of the harvested and extracted energy needs to be clear, as the extracted energy is not generally defined. The definition used in the present report for the extracted/harvested energy, is where the harvested energy is defined as the time integral of the power in the PTO force system times the cylinder velocity, hence, the extracted energy is for the simple model in this section given as;

$$E_{\text{har}}(t) = \int -f_{\text{PTO}}(t)\dot{z}_{\text{f}}(t)dt \tag{2.1}$$

Where f_{pto} is the PTO-force from the cylinder and $\dot{z}_f$ the cylinder velocity, which for the simple case is equal to the float velocity. The sign definition follows from the force and the float velocity must be opposite for energy to be harvested whereas equal signs indicated energy flow from the PTO-system to the waves through the float. Hence, energy is harvested when the PTO force is opposing the float movement.

With the incoming wave and the PTO force being periodic the energy extraction may be found as the energy extraction during one period multiplied by the number of periods. The energy extraction for a wave period is, hence, calculated by imposing the start and end of a time period as limits for the integral in Eq. (2.1). In Fig. 2.1.1 the float velocity is illustrated when a discrete PTO force is applied to a float in still water, where no incoming wave is imposed. The PTO force is seen in the upper graph whereas the float velocity due to the PTO force is seen in the lower graph. The middle graph shows the float velocity due to the first PTO box force applied in the first time period as if the PTO force in the following periods is set to zero.

One may notice that the float velocity at a given point is depending on the previous applied PTO force, therefore the velocity utilised to calculate the energy output is based on the PTO force applied in the current and the two previous time periods. Hence, to solve the velocity in one time period one needs the PTO force applied in the previously and the assumption of the incoming wave to be monochromatic. Here it is chosen to utilise the velocity induce by the PTO force in the previous two time periods since Fig. 2.1.1 indicates that velocity contribution form each box force is zero half way through the next time period. For the PTO system having three force levels as in Fig. 2.1.1 an analytical solution for the harvested energy may be found and graphically illustrated as a function of the force level and force width, see Fig. 2.3 (a). Hence, the energy harvested in one time period is plotted for varying box force level (F_1) and varying box force width (L_1). In Fig. 2.3 (b) and (c) the partial derivative of the harvested energy with respect to force level and force width is given respectively. The black lines indicates the nullclines, hence, the crossing of the black lines indicates the extreme points for the extracted energy.

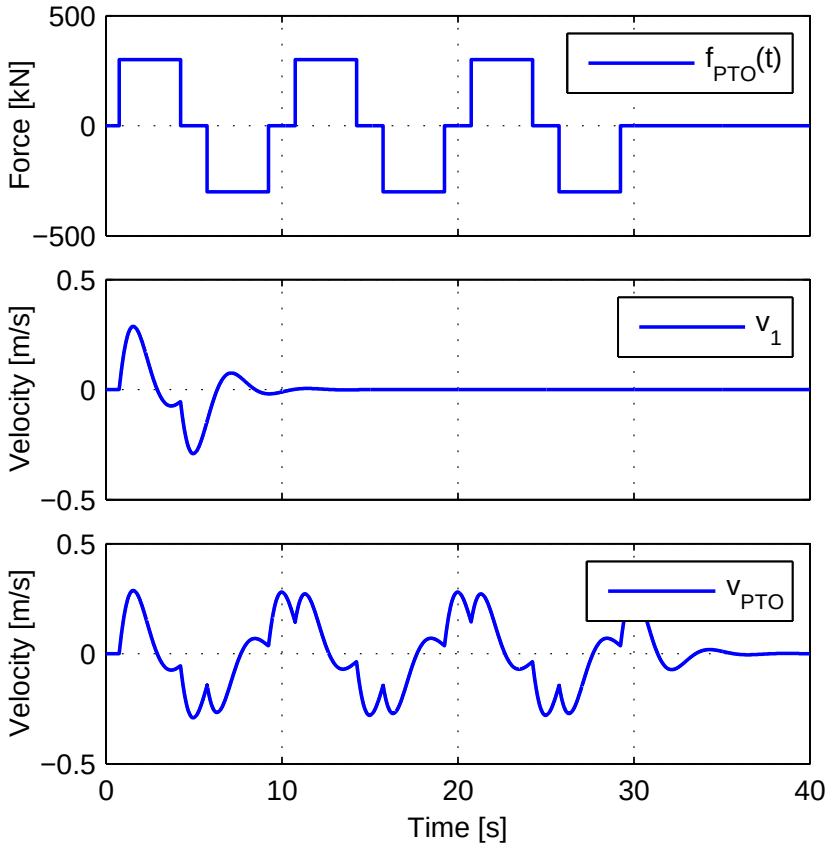

Figure 2.2: Illustration of float velocity when imposing a discrete PTO force.

The optimal configuration for a force profile with three force levels, working in monochromatic waves may hence be found analytically. The solution for maximal energy extraction is given graphically in Fig. 2.3 for a system with mass, damping and spring constants $m_\mathrm{f} = 1e5$ kg, $b_\mathrm{f} = 5e5$ Ns/m and $k_\mathrm{f} = 1e6$ N/m working in a monochromatic waves with amplitude and wave frequency $A_\mathrm{w} = 0.3$ m and $\omega_\mathrm{w} = \frac{1}{10}$ Hz.

Despite this simple system, the solution to the optimal force level and switch time is far from straightforward, and with the introduction of more force levels, the number of parameters to optimise (switch times a_i and b_i's and force levels F_i's, cf. Fig. 2.1) increases the analytical solution by orders of magnitude for the energy extracted. Therefore analytical optimisation of force profiles with more force levels is practically impossible. The remaining results presented are therefore made by employing time simulations and numerical optimisation routines.

2.1.2 Optimal Force Profile

As described above the optimal force for the discrete system may not be the same as for the continuous system. For the simple system given above an analysis has therefore been made to determine the force profile, which will yield the highest energy output to the grid. The optimisation of the force profile has here been carried out with two different objectives - either to maximise the energy extraction from the ocean

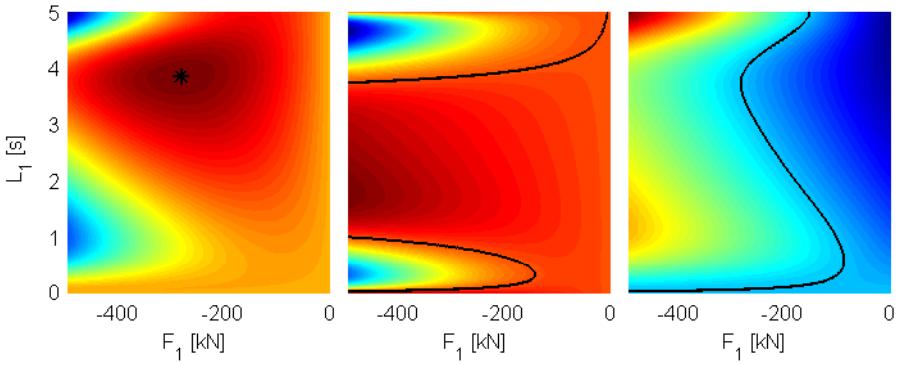

(a) (b) (c)

Figure 2.3: The graphical solution to the optimisation of the PTO force profile with three force levels. (a) Extracted energy. (b) Partial derivative of extracted energy with respect to force level. (c) Partial derivative of extracted energy with respect to force width.

waves or to minimise the force error to the continuous force, to see which yield the best results.

2.1.2.1 Optimisation to maximise harvested energy

With energy production as the overall objective for the WEC, the natural objective is to maximise the energy extraction from the ocean waves, hence the optimal force profile may be found from:

$$f_{\text{PTO.T}}(t) = \arg\min(-E_{\text{har}}(t)) \tag{2.2}$$

Hence, the problem is to identify the PTO force profile that yields the highest energy extraction. Note that the energy output is unmodelled in this simple model since a generic PTO force is applied.

2.1.2.2 Optimisation to best resemble the ideal continuous force reference

The second objective utilised in the force profile optimisation is to minimise the force error, whereby the optimal force profile may be found from:

$$f_{\text{PTO.T}}(t) = \arg\min(F_{\text{e}}(t)) \tag{2.3}$$

Where F_{e} is the force tracking error defined in (2.4). Hence, the discrete PTO force profile is optimised such that it tracks a continuous force reference with minimal error.

$$F_{\text{e}}(t) = |f_{\text{PTO.Cref}}(t) - f_{\text{PTO}}(t)| \tag{2.4}$$

The continuous force reference is generated with a reactive control algorithm utilising the float position and velocity as feedback, as:

$$f_{\text{PTO.Cref}}(t) = b_{\text{PTO}}\dot{z}_{\text{f}}(t) + k_{\text{PTO}}z_{\text{f}}(t) \tag{2.5}$$

With the coefficients b_{PTO} and k_{PTO} optimised for maximal energy extraction they are given as:

$$b_{\mathrm{PTO}} = b_{\mathrm{f}} \tag{2.6}$$

$$k_{\mathrm{PTO}} = m_{\mathrm{f}}\omega_{\mathrm{w}}^2 - k_{\mathrm{f}} \tag{2.7}$$

These parameters are found directly from the model of the wave-float interaction, cf. [14]. Notice that the coefficients are constant for a constant wave frequency.

2.1.2.3 Results with optimised force profiles

The optimised discrete force profile when utilising five force levels in a monochromatic wave is seen in the bottom of Fig. 2.4. The discrete PTO force are here compared with the optimal continuous force reference Eq. (2.5). The upper and middle plot gives the float position and velocity compared to the wave height and wave height velocity respectively.

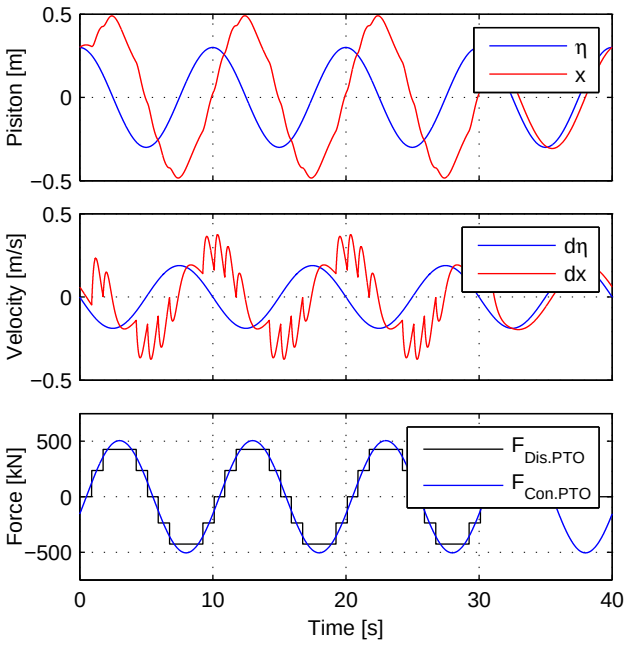

Figure 2.4: Illustration of float position and velocity with optimal discrete force profile and a monochromatic incoming wave.

Note that the PTO force enforces the float movement to be larger than the wave height, hence resonance is obtained as with the optimal continuous control. Note however, that the PTO force is optimised so the maximum energy is extracted from the waves. Hence, the operation point imposed by this control may dramatically degrade the conversion efficiency when implemented in a practical PTO-system where imperfect conversion is employed. The optimal discrete PTO force profile is seen to be close to equal to the continuous force reference.

In Fig. 2.5 (a) the optimal PTO force profiles are given for a system utilising five force levels working in three different wave heights but with the same wave frequency. In Fig. 2.5 (b) the optimal force profile for

a system utilising 3, 5 or 7 force levels are given when working in the same monochromatic wave. As one would expect larger waves calls for larger PTO forces. Further it is seen that the timing of the force shifts are unchanged with the increasing wave heights when utilising a fixed number of force levels (a). However, both the timing and size for the forces differ for systems with various numbers of force levels (b).

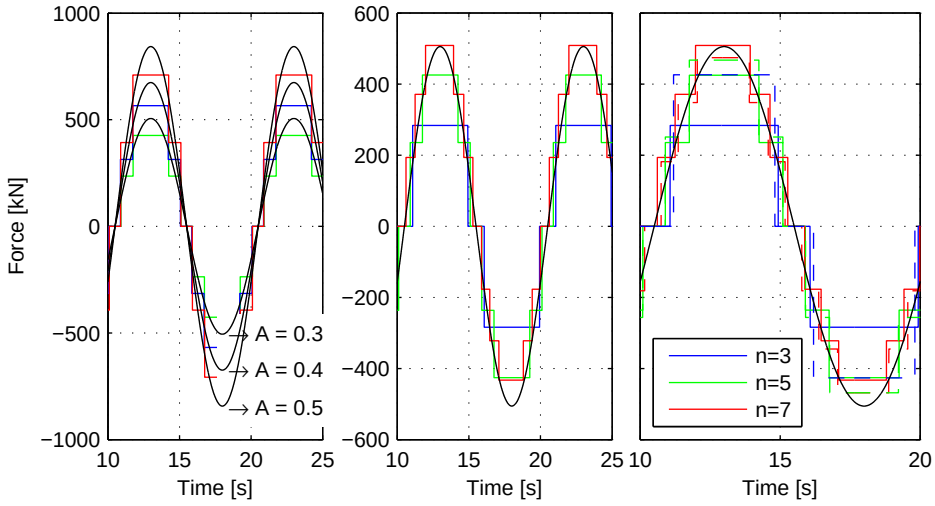

Figure 2.5: Optimal discrete force profiles. (a) For varying wave input and five force levels. (b) 3,5 or 7 force levels for fixed input wave. (c) Energy(solid) and force error(dashed) optimised force profiles. Note; the force axis for (b) and (d) are equal.

The force error and energy optimised force profiles are compared in Fig. 2.5 (c). It is seen that with an increasing number of force levels, the two objective functions result in more equal optimal force profiles.

In a physical discrete force system the number and size of forces may not easily be changed, why a fixed number of forces must be chosen. However, the on and off timing, i.e. when switched from one value to the next, of these forces may still be optimised. In Fig. 2.6 the optimal force profiles are given for a system with seven force levels when operating in waves with varying amplitude. Note how the need for a smaller force is met by imposing a shorter on time for the large force and even refraining from using the maximum force level in some situations. This way the force profile is fitted to the need by fitting the on time for each force level.

In table 2.7 the energy extraction is compare for a system working with a fixed number and size of force levels where the timing is optimised.

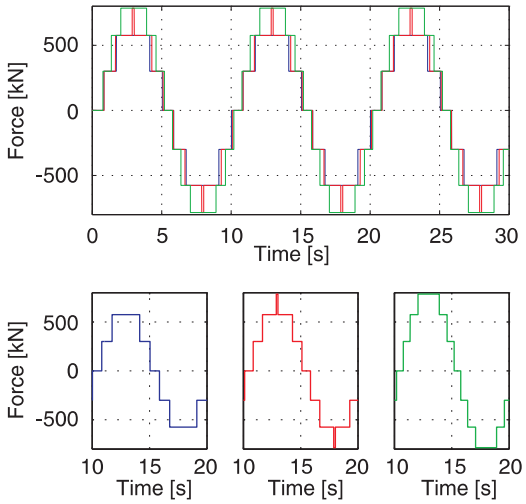

Figure 2.6: Optimised force profiles with fixed number of available force levels

Wave		Number of Forces		
A_w	ω_w	3	5	7
0.3	$\frac{2\pi}{10}$	66.8	60.7	81.1
0.4	$\frac{2\pi}{10}$	64.2	89.5	92.2
0.5	$\frac{2\pi}{10}$	58.2	90.6	97.4
0.5	$\frac{2\pi}{5}$	87.5	95.2	98.3
0.5	$\frac{2\pi}{3}$	96.6	99	98.7

Figure 2.7: Normalised extracted energy in % during one wave period, utilising fixed force levels and optimised force shapes. The energy extraction is normalised with the energy extraction by a optimal continuous force system.

2.1.3 Discrete Force Profile

Based on the investigation of the discrete force profile for a generic PTO force system utilised for a simple heave motion point absorber it was hereby found that:

- the size of the optimal force is highly influenced by the size of the incoming wave whereas the timing is depending on both the wave frequency and the wave height.
- it is seen that a reasonable energy extraction may be obtained with 7 fixed force levels even for varying sea conditions when the on and off switching of the force is optimised.
- the analytical approach imposing the symmetric and periodic nature of the PTO force profile is inadequate when irregular waves are examined.
- despite no losses in the PTO-system have been included, the results for the monochromatic waves indicate that tracking the optimal continuous force reference is reasonable and that relative few force levels are needed.

In the following sections the results for the case, where the analysis has been extended to include irregular waves and a simulation model including a generic model of the discrete fluid power force system are therefore presented. The results hence include the losses in the switching manifold. Before presenting these results the algorithms for selecting a force levels and when to switch between different forces are first presented.

2.2 Force Shift Algorithms

The choice of which force to apply is performed with a Force Shift Algorithm (FSA). The force control algorithms which have been utilised are divided into a general FSA and a valve control algorithm for the

bidirectional check valves which has been considered (these are discussed in chapter 3). The valve control algorithm is used to determine whether the valve is to perform active or passive switching for a given force shift. The on/off valves are controlled solely based on the FSA.

Based on the system configuration, (selection of working areas and pressure lines) a force vector, $\bar{F}_{\text{vec}}$, containing the applicable forces is constructed. A force error for the discrete force have then been defined as:

$$F_{\text{e}}(k) = F_{\text{PTO.ref}}(t) - \bar{F}_{\text{vec}}(k) \tag{2.8}$$

With $F_{\text{PTO.ref}}$ being the PTO force reference. The force error when applying force number k is then given by $F_{\text{e}}(k)$.

FSA-I

Based on the results in section 2.1.2, the first force shift algorithm is developed to minimise the force error and is given by;

$$k = \arg\min\{|F_{\text{e}}(k)|\} \tag{2.9}$$

Hence, the force combination leading to the smallest force error, $F_{\text{e}}(k)$, is chosen.

FSA-II

The second FSA is given by;

$$k = \arg\min\{|F_{\text{e}}(k_-)|, |F_{\text{e}}(k_0)|, |F_{\text{e}}(k_+)|\} \tag{2.10}$$

$$k_- = \arg\min_{k\in S_-}\{E_{\text{sw}}(k)\} \ , S_- = \{k \,|\, F_{\text{PTO.ref}} - F_{\text{b}} < \bar{F}_{\text{vec}}(k) < F_{\text{PTO.ref}}\} \tag{2.11}$$

$$k_+ = \arg\min_{k\in S_+}\{E_{\text{sw}}(k)\} \ , S_+ = \{k \,|\, F_{\text{PTO.ref}} < \bar{F}_{\text{vec}}(k) < F_{\text{PTO.ref}} + F_{\text{b}}\} \tag{2.12}$$

However, if

$$S = S_- \cup S_+ = \emptyset \tag{2.13}$$

$$k = \arg\min\{|F_{\text{e}}(k)|\} \tag{2.14}$$

$E_{\text{sw}}(k)$ is a function describing the switching loss associated with a force shift from the current force to the force k, see Eq. (2.15).

The control furthermore includes a minimum on-time for each force to reduce chattering. During the investigation of energy production this minimum on-time, T_{minOn} is set to 350 ms. The force band is set to, $F_{\text{b}} = 150$kN. The settings of the minimum on-time and the force band have been determined based on time series simulations, for which the results may be found in papers B and C. Setting F_{b} too high will impose poor force tracking while a low value of F_{b} will impose a large number of switchings. An illustration of FSA-II is given in Fig. 2.8. Note that at the time instant of a force shift, the algorithm may only chose a force level within the grey force band $\pm F_{\text{b}}$. Furthermore the algorithm chose the force within the grey force band leading to the smallest energy loss $E_{\text{sw}}(k)$. Hence, the force error is not minimised, see e.g. the red line. Here the force error could be significant lower, however the lower force level is chosen since it leads to the smallest switching loss $E_{\text{sw}}(k)$.

The pressure line which a given cylinder chamber should be connected to is hence based on Eq. (2.9) or (2.10). The inevitable energy loss associated with a force shift is the sum of losses due to the pressure shifts

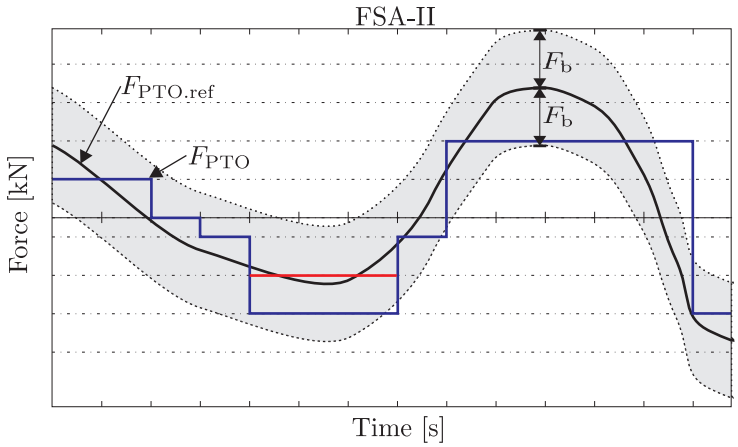

Figure 2.8: Illustration of FSA-II. The horizontal lines indicates the applicable force levels.

performed in each cylinder chamber. The switching loss is thus given as:

$$E_{\mathrm{sw}}(k) = \sum_{i=1}^{i=n} \frac{V_i}{2\beta} \left(p_{\mathrm{c}.i}(k_0) - p_{\mathrm{c}.i}(k)\right)^2 \tag{2.15}$$

Where k_0 indicates the current force applied and k indicates the force being switched to. As apparent from (2.15) the energy loss associated with a force shift depends on the size of the pressure change and on the size of the volume. Consequently a given force shift may lead to various energy losses accordingly to the piston position, why the switching loss is and has to be calculated online in the controller.

2.3 Background for Evaluating Configuration Results

As background for investigating the optimal system configurations a generic model of the discrete PTO-system has made, the details of which may be found in [8]. The model has here been constructed, so the number of working areas and pressure lines may easily be changed, to represent different configurations of the system. The discrete fluid power force system is evaluated by implementation in a single float point absorber WEC simulation model of the Wavestar. Hence, the discrete PTO-system model is combined with a float and wave model, so the PTO-system may be evaluated when implemented in a WEC operating in irregular waves. In Fig. 2.9 an illustration of the combined system is given. The model includes irregular wave modelling, wave-float interaction and the primary stage of the discrete fluid power force system. This model is hence the basis of the analysis and results presented in the following sections.

The wave-float interaction model is based on linear wave theory and the point absorber being small compare to the wave length. The wave-float interaction model utilised is described by Hansen and Kramer in [14]. However, when comparing various system configurations three fixed wave times series are utilised whereby equal inputs are experienced by the systems under comparison. The three wave series resemble three sea conditions, small, medium and large waves relative to the wave climate at Hanstholm, a previous Wavestar test site. The wave climate at Hanstholm is given by the scatter diagram in Tab. 2.1. The wave climate is given by the wave significant height ($H_{\mathrm{m},0}$) and the mean wave time period ($T_{0,2}$). The significant wave height is often defined as the mean wave height (trough to crest) of the highest third of the waves. The three

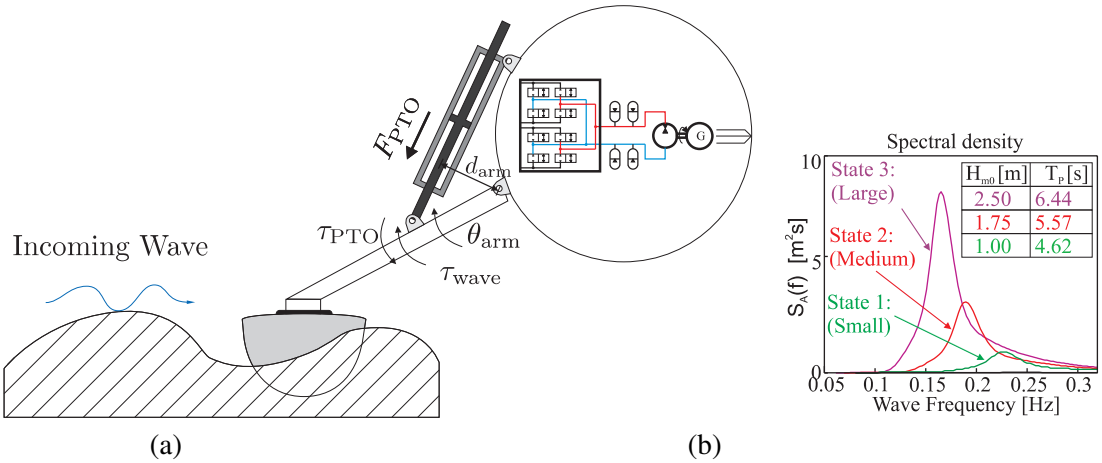

Figure 2.9: Illustration of single float point absorber model with discrete fluid power PTO system and the wave density spectrums utilised for the three sea states.

sea states utilised in the modelling are marked in boldface blue in Tab. 2.1 and their density spectrums are given in Fig. 2.9 (b). One may note that the C5 machine installed at Hanstholm is in production for waves in the range of $H_{m.0} = [0.5 - 3.0]$.

$H_{m,0}$	Mean wave period $T_{0,2}$[s]							Sum
[m]	2-3	3-4	4-5	5-6	6-7	7-8	8-10	[%]
0.0 - 0.5	2.65	8.18	1.84	0.38	0.14	0.03	0.01	13.2
0.5 - 1.0	1.22	**19.2**	11.4	2.21	0.18	0.06	0.02	34.4
1.0 - 1.5	0.00	**6.84**	13.0	2.96	0.30	0.04	0.00	23.2
1.5 - 2.0	0.00	0.33	**9.58**	3.05	0.29	0.04	0.00	13.3
2.0 - 2.5	0.00	0.02	3.34	**4.60**	0.20	0.04	0.00	8.20
2.5 - 3.0	0.00	0.01	0.22	**3.89**	0.21	0.01	0.01	4.40
3.0 - 3.5	0.00	0.00	0.00	1.38	0.51	0.01	0.01	1.90
3.5 - 4.0	0.00	0.00	0.00	0.17	0.57	0.02	0.01	0.80
4.0 - 4.5	0.00	0.00	0.00	0.00	0.24	0.07	0.00	0.30
4.0 -	0.00	0.00	0.00	0.00	0.07	0.21	0.06	0.30
Sum[%]	3.87	34.6	39.5	18.6	2.72	0.52	0.16	100

Table 2.1: Scatter diagram for Hanstholm pear. The sea state utilised ($H_{m,0}$,$T_{0,2}$), SSI: (1m, 3.95s). SSII: (1.75m, 4.76s). SSIII: (2.5m, 5.50s) [14]

2.4 Results for Individual Analysis of Pressure Lines, Chambers and Pressure Levels

Although the optimal number of pressure lines, the number of cylinder chambers and the areas of these directly couple to each other in the optimal configuration, a simplified analysis has been made to analyse the influence of each of these parameters, while the others are kept constants. The results of this analysis

is presented in the following and is the background for the results of the complete system configuration and analysis presented in the next sections. The section is based on the results presented in paper B and C, which may be referenced for further details.

2.4.1 Optimal Number of Pressure Lines

The first results are based on the varying the number of pressure lines, while keeping the number of cylinder chambers to two. This has been done, as standard cylinders are two chamber versions, where multi-chamber cylinders in general are much more complex in nature and hence suffer from poorer reliability. In the analysis the pressures in the pressure lines are equally distributed between 20 and 250 bar, depending on the number of pressure lines, i.e. for two pressure lines the pressures are $\begin{bmatrix} 20 & 250 \end{bmatrix}$bar, whereas it for three pressure lines are $\begin{bmatrix} 20 & 135 & 250 \end{bmatrix}$bar and so forth. The cylinder efficiency is not accounted for and the valve dynamics are for the first results neglected. FSA-II is used for the results presented and sea state II is used. For further details, please refer to paper B. Based on these assumptions, the simulation results for a case with four pressure lines are shown in Fig. 2.10.

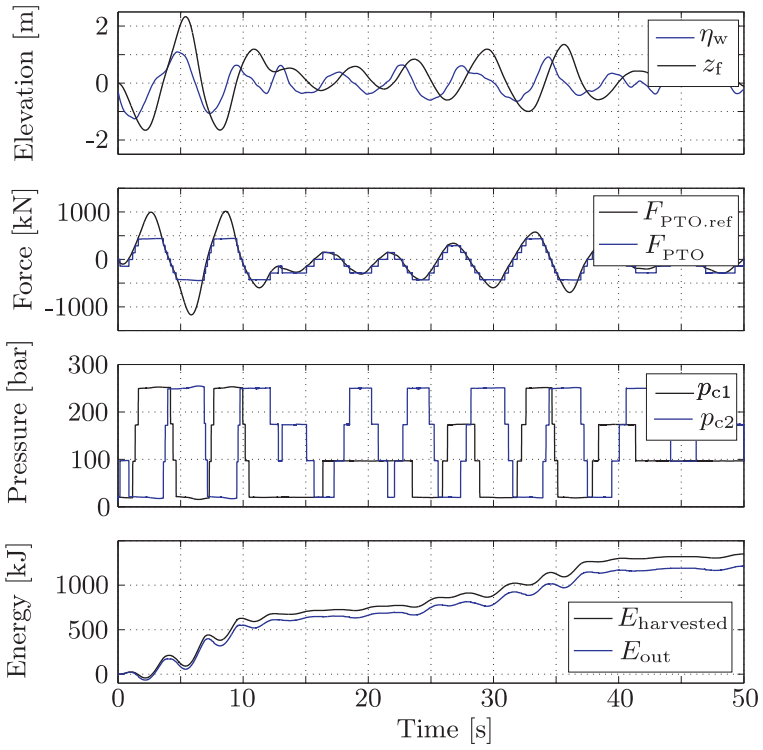

Figure 2.10: The first window shows the horizontal wave and float elevation, the second the continuous force reference and the discrete force sought to track the reference. The third plot shows the cylinder chamber pressure, and the last plot shows the harvested energy along with the energy output to the common pressure lines.

The first window here show the wave heigh and the float position, the second window the force reference and actual force. The third window show the pressures in the two chambers and the forth window show the harvested and output energy of the system. In the figure it is seen how the chamber pressures varies between

four pressure levels as the PTO force steps through the seven obtainable forces seeking to track the PTO reference force. The energy output is used for calculation of mean power output. From the simulations the float movement is seen to exceed the wave height, this is due to the nature of reactive control that is designed to enlarge the float movement. The discrete PTO force is seen to track the PTO force reference fairly well when the reference due not exceed the maximum discrete force which is determined based on the piston area and the maximum pressure in the common pressure lines. The pressure in the two chambers that generates the discrete PTO force are seen to have opposite size when a large force is needed, hence a large pressure difference is present. The discrete steps in the PTO force are not noticeable on the float position, this is due to the filtering effect of the large inertia of the float. Based on the above, the power output have been analysed as a function of the number of pressure lines. The results of which are seen in Fig. 2.11.

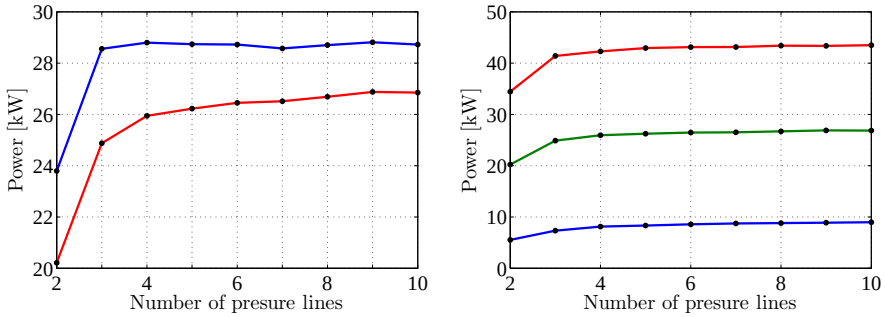

Figure 2.11: Left: Harvested(blue) and Output(red) mean power in Sea State II. Right: Mean power output, for Sea State I(Blue), II(Green), III(Red). Both left and right with infinitely fast valve dynamics and force band and minimum on time optimised for power output. FSA-II was used.

From these graphs it may be seen that increasing the number of pressure lines from two to three has significant impact on both the harvested and output power. However, including further pressure lines only have minor influence on the results, relative to the increase in the number of pressure lines. Almost the same results are obtained if including the valve dynamics in the analysis, as presented in Fig. 2.12, where a valve with 16 ms opening time has been included.

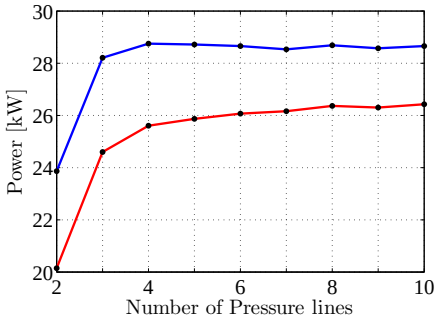

Figure 2.12: Harvested (blue) and Output (red) mean power in Sea State II. Valve opening time is 16[ms] and a the valve dead time has been optimised to 8[ms]. The force band and the minimum on time are optimised for each pressure line set-up. FSA-II was used.

Based on these results it is therefore found that increasing the number of pressure lines increases the power supplied to the common pressure lines. Furthermore the results suggest that by use of faster valves the power

production is increased. Practically there will however be limitations on what is physically feasible, and results therefore indicate that the optimal number of pressure lines is close to three or four, as little is gained by increasing this number further.

2.4.2 Optimal Number of Cylinder Chambers and Areas

The second part of the sub-analysis is made, where the number of pressure lines is two, with fixed pressures, but where the number of cylinder chambers are varied and so is the areas related to the different chambers. This is illustrated in Fig. 2.13, which shows respectively a two chamber cylinder and a three cylinder chamber. The areas refers to the cross-sectional areas of the piston minus rod, i.e. A_1, A_2 and A_3 in the figure. In the following, a "negative area", refers to an area, on which the pressure works in the opposite direction of the piston movement x_p.

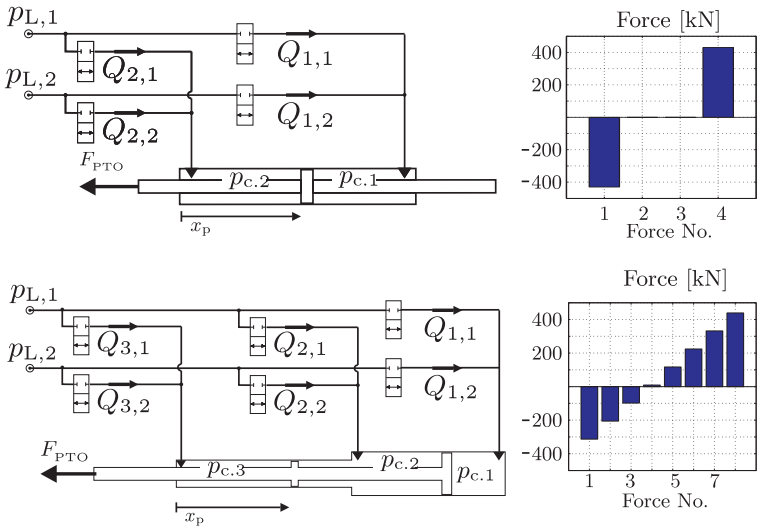

Figure 2.13: Examples of the discrete hydraulic force system and the force combinations when utilising an binary area coding.

Three different ways of encoding the areas, i.e. setting the size of the areas relative to each other, have been considered these are:

Binary encoding 1: The first area coding strategy has one working area applying force in positive direction, A_1. The areas in the negative direction are binary half's of the area in positive direction. Hence, each time an extra area is introduced its size is half of the smallest in the negative direction. This is the encoding illustrated in Fig. 2.13. The basic area chosen is $A_1 = 190\ \text{cm}^2$, which is similar to the area found on the symmetric cylinder used by the Wavestar WEC today.

Binary encoding 2: The second binary encoding follows the area distribution utilized by Linjama et. al in [17]. In this encoding the first area is in positive direction, the second area is in negative direction and is half in size of the first, the third area is in positive direction and is half in size of the second an so forth.

Optimised encoding: The optimised encoding refers to an area encoding, where the different areas are optimised particularly for a given sea condition using a standard optimisation algorithm to maximize the energy output.

With these encodings the influence the number of chambers and the areas of these may be analysed. The results of this analysis are presented in Fig. 2.14 and the areas using the optimised encoding are shown in Fig. 2.15.

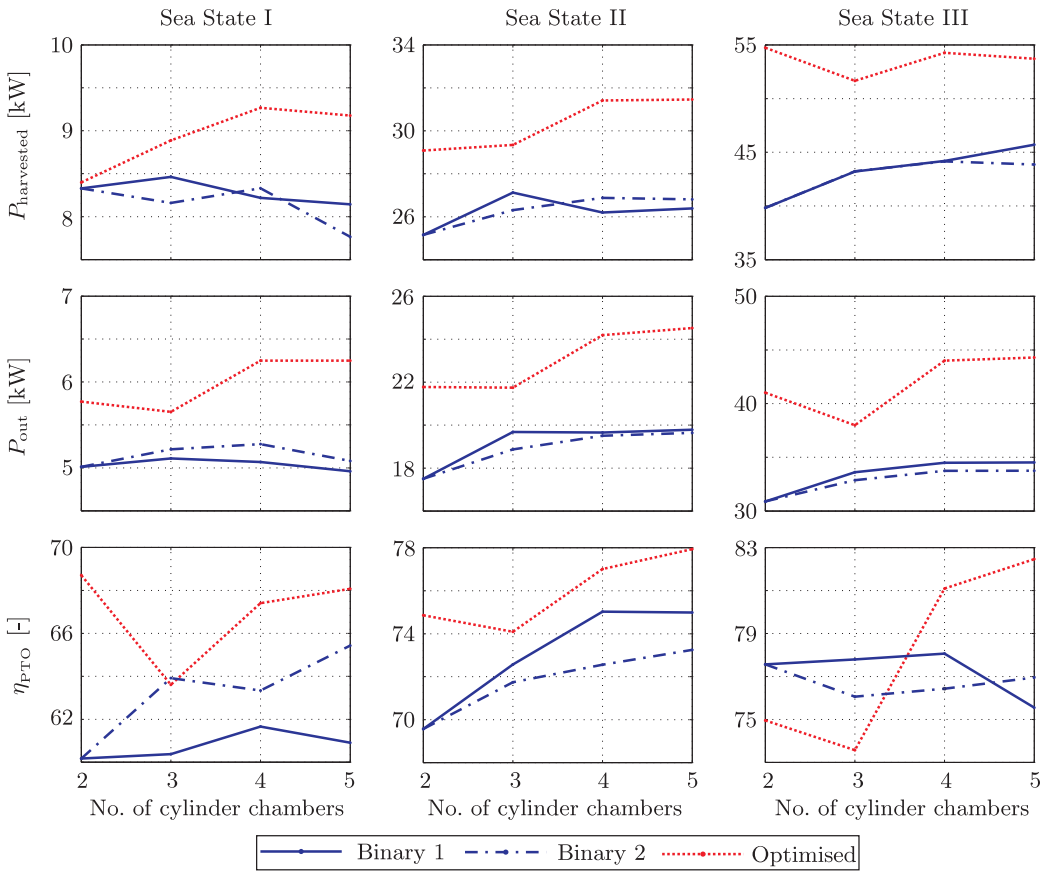

Figure 2.14: Simulation results, each column represents a sea state. The upper row is the harvested power, middle row is the output power to the pressure line, and the lower row is the efficiency of the primary PTO stage.

From the simulation results it is seen that the optimised area encoding strategy is the one leading to the highest power output for all sea states. It is seen that the efficiency is higher and that the number of valve actuations are lower for the optimised area encoding compared to the two binary encoding strategies in most situations, which may have positive impact on the lifetime of the valves. Hence if only operating in a single sea state the optimised area distributions will perform better than the binary. However, as is apparent from Fig. 2.15, then the optimised areas changes significantly dependent on the sea state, but where the relative changes for a given area becomes smaller, when increasing the number of chambers. From the results it may also be seen that overall the optimised configuration with four working areas may be preferred as increasing to five do not imply significant improvement. However it should be noted that the system configurations

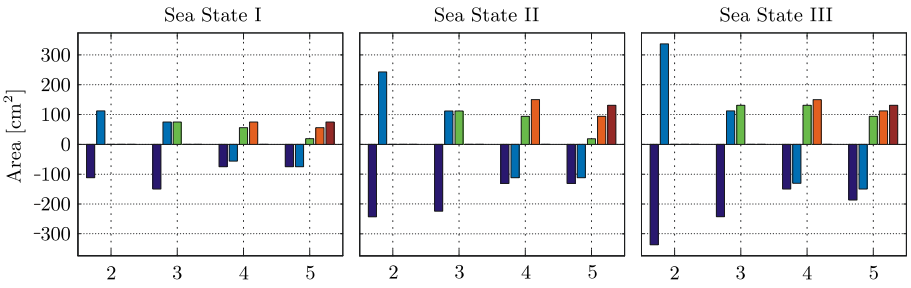

Figure 2.15: Optimised areas for the different sea states and as function of the number of chambers.

		Sea State		
Configuration	n	I	II	III
Binary 1	2	1.37	2.22	2.47
Binary 2	2	1.37	2.22	2.47
Optimised	2	1.23	1.11	1.49
Binary 1	3	1.78	3.08	3.53
Binary 2	3	1.58	2.88	3.87
Optimised	3	1.45	1.94	3.18
Binary 1	4	2.15	2.97	4.52
Binary 2	4	2.07	3.48	4.53
Optimised	4	2.33	2.55	3.13
Binary 1	5	2.60	3.64	7.16
Binary 2	5	2.17	4.00	5.19
Optimised	5	2.50	3.00	3.03

Table 2.2: Number of valve actuations per second for various sea states and area encoding.

for the binary strategies are unchanged over the sea states contrary to the optimised strategy. Hence, for a more realistic comparison a single optimised area distribution should be chosen for all sea states, as the multi-chamber cylinder is not changed for various sea conditions. This is done in the next section, where results when optimising the complete system configuration is considered.

2.5 System Configurations

Based on the above results the results from a complete system configuration and optimisation have been developed. For the generic simulation model two parameter sets, U_{PL} and U_{A} holding various system configurations have been constructed and used as inputs to the simulation model. Based on the above presented results it was chosen to utilise systems with two or three pressure lines in combinations with multi-chamber cylinders with two or three cylinder chambers for the brute force optimisation. The set, U_{PL}, of pressure line combinations are constructed so the low pressure line always is 20 bar, no pressure lines have equal value, and the maximum pressure setting is 260 bar. The pressure line set is given as:

$$U_{\mathrm{PL}} = U_{\mathrm{P2}} \cup U_{\mathrm{P3}} \tag{2.16}$$

Where the subset for two and three pressure lines are given as:

$$U_{\mathrm{P2}} = \left\{ \begin{array}{c|c} P_{\mathrm{L}} & \left\{ \begin{array}{c} 20 \\ 20+30l_1 \end{array} \right\} \text{ for } l_1 = \{1..8\} \\ P_{\mathrm{H}} & \end{array} \right\} \tag{2.17}$$

$$U_{\mathrm{P3}} = \left\{ \begin{array}{c|cc} P_{\mathrm{L}} & \left\{ \begin{array}{c} 20 \\ 20+30l_1 \\ 20+30l_2 \end{array} \right\} & \begin{array}{c} l_1 = \{1..7\} \\ \text{for } \ l_2 = \{2..8\} \\ l_1 < l_2 \end{array} \\ P_{\mathrm{M}} & & \\ P_{\mathrm{H}} & & \end{array} \right\} \tag{2.18}$$

Where the minimum pressure difference between adjacent lines is set to 30 bar.

For the working areas the set, U_{A}, is constructed such that, the cylinder is symmetric, the maximum and minimum size of a working area is 420 cm^2 and 21 cm^2 respectively, which corresponds to a full circle with diameter of approximately 23 cm and 5 cm. The area set is given as:

$$U_{\mathrm{A}} = U_{\mathrm{A2}} \cup U_{\mathrm{A3}} \tag{2.19}$$

Where the subset for two and three working areas are given as:

$$U_{\mathrm{A2}} = \left\{ \begin{array}{c|c} A_1 & \left\{ \begin{array}{c} a_1\hat{A}_{\max} \\ -a_1\hat{A}_{\max} \end{array} \right\} \text{ for } a_1 = \{1,2..20\} \\ A_2 & \end{array} \right\} \tag{2.20}$$

$$U_{\mathrm{A3}} = \left\{ \begin{array}{ll|c} A_1 = & a_1\hat{A}_{\max} & a_1 = \{2..20\} \\ A_2 = & -a_2\hat{A}_{\max} & a_2 = \{1,2..19\} \\ A_3 = & (a_2-a_1)\hat{A}_{\max} & a_1 > a_2 \end{array} \right\} \tag{2.21}$$

Where the factor $\hat{A}_{\max}$ is a measure for the resolution used in the analysis and is given as:

$$\hat{A}_{\max} = \frac{A_{\max}}{20} = 21 \text{ cm}^2 \tag{2.22}$$

With these pressure line and cylinder area sets given, a number of systems defined by the pressure lines (PL) and the areas (AP) may be generated for the analysis. Examples of these pressure sets and areas sets are:

$$PL(l_1 = 6) = [20\ 200] \text{ bar} \tag{2.23}$$

$$PL(l_1 = 1, l_2 = 3) = [20\ 50\ 110] \text{ bar} \tag{2.24}$$

Likewise for the cylinder areas;

$$AP(a_1 = 1) = [21\ -21] \text{ cm}^2 \tag{2.25}$$

$$AP(a_1 = 10, a_2 = 4) = [105\ -84\ -126] \text{ cm}^2 \tag{2.26}$$

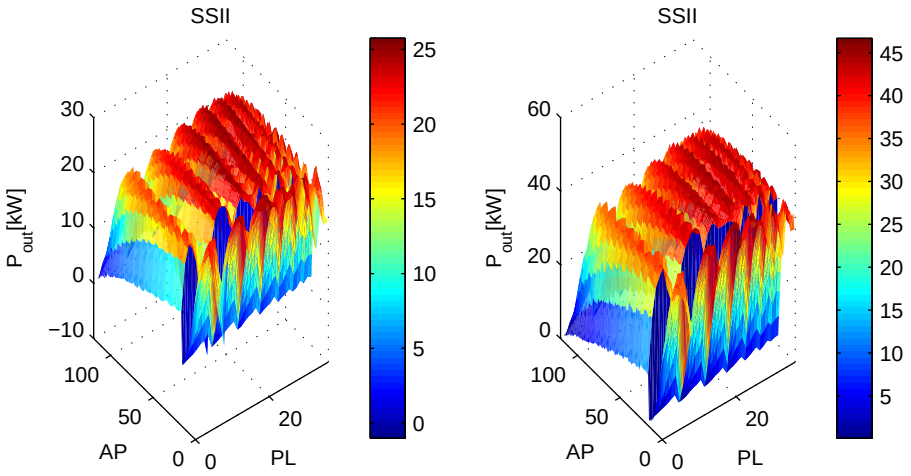

Figure 2.16: Average power output to the common pressure lines in sea state II and III. The pressure lines and area vectors (PL and AP) are given in section 2.5.

2.6 Optimal System Configuration

The discrete nature of the discrete PTO system configuration leads to a large number of local optima why a brute force optimisation approach is employed, as traditional optimisation techniques would get stuck. Hence, the energy extraction from with each system combination defined above (PL(n1) and AP(n2)) is found through simulations. The performance for each system is calculated for the WEC when exposed to each of the three sea states, see Fig. 2.16 for average power output in sea state II and III (Extracted power, output power and conversion efficiency in the three sea states may be found in paper D). The axes AP and PL indicates the various multi-chamber and pressure line configurations respectively.

With these solution sets of average extracted and output power for each system configuration in the three sea states one may chose the system configuration yielding the best performance. Best performance is here depending on the objective; highest energy extraction, highest energy output or highest conversion efficiency.

A WEC installation site may be represented by a scatter diagram holding the time distribution of wave conditions for the given site, as seen in Tab. 2.1. One may see T_{sea} in (2.27) as a very simple representation of the scatter diagram, where T_{sea} indicates time distribution between sea state I, II and III, as:

$$T_{\text{sea}} = [T_{\text{SS1}}\ T_{\text{SS2}}\ T_{\text{SS3}}] \tag{2.27}$$

Naturally one could include more sea states in T_{sea}, however, with a corresponding significant increase in computation time of the optimisation. T_{sea1} and T_{sea2} are utilised as examples where the optimal system configuration is desired for these two site conditions.

$$T_{\text{sea1}} = [0.8\ 0.1\ 0.1] \tag{2.28}$$
$$T_{\text{sea2}} = [0.1\ 0.7\ 0.2] \tag{2.29}$$

The objective function maximising the energy output to the common pressure lines is chosen, so the system

configuration vectors may be given as:

$$(\underline{A}_{\mathrm{p}},\ \underline{P}_{\mathrm{L}}) = \arg\max\left(\Sigma_{SS=1}^{3}\left[\bar{P}_{\mathrm{out}}(\underline{A}_{\mathrm{p}},\ \underline{P}_{\mathrm{L}}, SS)T_{\mathrm{sea}}\right]\right) \tag{2.30}$$

By utilising method, the optimisation hence gives the piston areas for the multi-chamber cylinder and the common pressure lines leading to the maximal average power output to the common pressure lines in the sea conditions given by the time distribution T_{sea}. In Fig. 2.18 the average power extraction and average power output to the common pressure lines are given for the two site conditions T_{sea1} and T_{sea2} respectively. Furthermore the conversion efficiency is given. The results are plotted as "functions" of the system configuration, hence, the configuration of the multi-chamber cylinder and the common pressure lines.

As expected the discrete nature of the system imposes several local optima. It is seen that the surfaces are arranged in mountain chains and valleys. Due to the difference in sea condition applied by T_{sea} a significant difference is seen in energy results for the two columns. The optimal configuration for the two sea conditions T_{sea1} and T_{sea2} in term of maximal average power output to the common pressure lines are given in table 2.3. Note, that both configurations consists of a three chamber cylinder and three common pressure lines.

	A_{p} [cm^2]	p_{L} [bar]
T_{sea1}	[−273 105 168]	[20 140 230]
T_{sea2}	[−357 147 210]	[20 110 170]

Table 2.3: Optimal system configuration for T_{sea1} and T_{sea2} when optimised for maximal average power output in each wave condition.

2.7 Discussion of System Configuration

From the above results it should be clear that the configuration of the discrete fluid power force system highly affects the performance of the WEC. It is clear that the number of cylinder chambers and pressure lines entails the number of applicable forces, and that the size of the piston area and the pressure level dictates the size of the forces.

In Fig. 2.17 the normalised average power output to the common pressure lines are given for all the system configurations in each sea state. The normalisation is performed with respect to the maximal average power output,

$$\bar{P}_{\mathrm{out.Nom}}(AP(i), PL(j)) = \frac{\bar{P}_{\mathrm{out}}(AP(i), PL(j))}{\max\left(\bar{P}_{\mathrm{out}}(\underline{AP}, \underline{PL})\right)} \tag{2.31}$$

Hence, this indicates the performance of a system configuration within a given sea state. It is clearly seen how the optimal configuration differ from sea state to sea state. From Fig. 2.17 it may been seen how one may choose a symmetric cylinder ($AP = [1\ 19]$) and still reach a good power output. However, if one needs to choose one symmetric cylinder usable in all sea state the pressure levels have to be adjustable to reach high power output in all sea states. Adjustable pressure lines may though not be suitable since the accumulator capacity requirements will increase significantly. Similarly, as the energy losses resulting from switching the pressure in a cylinder chamber is proportional to the square of pressure change and proportional to the volume, the possibility to introduce extra or larger force levels by adding extra pressure lines or cylinder

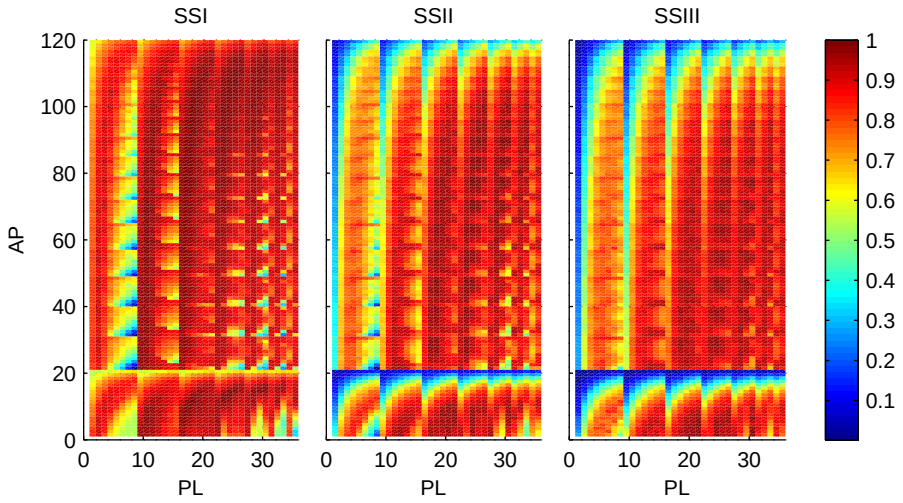

Figure 2.17: Energy Output for in the three sea states, normalised with the maximum energy output for the given sea state.

chambers, may benefit to increase the conversion efficiency. This study is, however, only related to the theoretical results, and practical issues are not considered. Yet introduction of an extra pressure line may require larger effort throughout the entire machine, and requires an extra set of valves in the switching manifold. Similar increasing the number of chambers in a cylinder, will also require extra valves in the manifold and may also add further to the complexity of the cylinder. For a given system practical matters therefore also has to be taken into account.

The studies in this chapter shows that numerous system configurations leads to a high energy production, however, it was also shown that numerous system configurations lead to a low energy production. Through the investigations it is seen that an analytical optimisation of the system configuration is infeasible when optimising for energy production in irregular waves. The method utilising time series simulations incorporates the sea state time distribution given by the wave climate at a given installation site. It was shown that the time distribution of the sea state highly influence which system configuration leads to the highest energy production. Hence, one must carefully chose the system configuration based on the wave climate at the installation site, and this may be done based on the method outline above and in detail in [8].

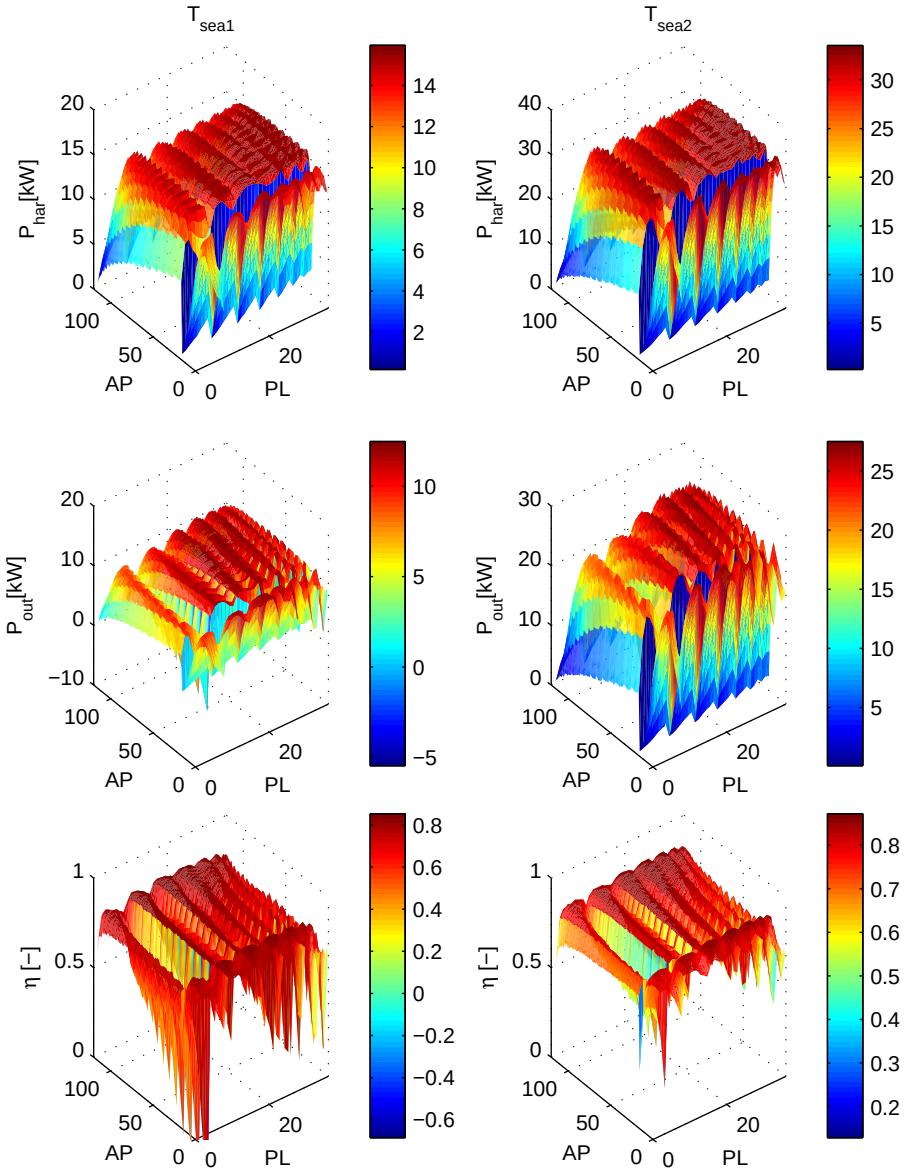

Figure 2.18: Average extracted and output power along with the conversion efficiency for the site conditions T_{sea1} and T_{sea2} in left and right column respectively. The pressure lines and area vectors (PL and AP) are given in section 2.5.

Chapter 3

Valves and Switching Manifold

The primary stage of the discrete fluid power force system consists of a multi-chamber cylinder, multiple common pressure lines and a switching manifold. The switching manifold is the controlling element in the force system, which control the force by controlling which of the common pressure lines are applied to each cylinder chamber. Hence, the valves in the switching manifold control the system, not by throttling but by controlling flow directions. As described in the previous chapter a valve opening inevitable introduces an energy loss when changing the pressure in a fixed volume. However, if the volume is changing in size the valve opening area influence the energy loss since a throttling loss due to displacement flow occurs in addition to the compressibility loss.

The timing of the disconnection and connection of pressure lines and cylinder chamber affects the pressure in the cylinder chamber, especially if the cylinder chamber volume is changing. If a chamber is cut off from all pressure lines for too long a period, the pressure may increase or decrease inappropriately. Alternatively connecting two or more pressure lines at the same time on the other hand leads to significant short circuit flow and substantial energy losses. Hence, both timing of disconnection and connection of the pressure lines and the valve switching time have influence on the energy loss in the switching manifold. The timing between disconnection and connection of the pressure lines is a control issue which is dependent on the valve switching time, the volume gradient, chamber pressure and the fluid compressibility. The valve switching time is on the other hand a design issue, for the valve designer. For this reason this different valve concepts are considered in the present chapter. This includes the design considerations which relate to different on-off valve concepts which have been investigated, but also considerations regarding the conceptual design of bi-directional check-valves are addressed, as these may eliminate some of the timing issues in the control.

One of the main challenges in the valve design and for the switching manifold is to obtain large scale valves (flow rates >600 l/min at low pressure drop), with a sufficiently fast switching time (around or below 15 ms). Different valve concepts have therefore been developed and investigated. This includes the design of an on-off valve utilising a Danfoss Power Solutions PVX-pilot valve (referred to as the PXE), the specifications for a prototype valve, which is being developed by Bucher Hydraulics, but also the conceptual design of a multi-poppet valve, which fulfils the design requirements. The original plan in the project was partly to investigate possible on-off valve solutions based on Danfoss Power Solutions products, but as these do not have a direct type valve suited for the given application, the development of a valve was also initiated with Bucher Hydraulics, based on the specifications developed in the current project. The status for this progress is that the valve by Bucher Hydraulics is still under development and prototype testing at Bucher, why this has not been tested on the wave simulator test bench set-up (described in the next chapter). The development

of the Bucher valve is based on the same specifications as for the valve developed based on the PXE-pilot valve, the design of which is described in the next section. Due to the limitations with this process other conceptual valve solutions have also been investigated, which is described afterwards, which has also lead to the considerations to utilise bi-directional check-valves alternative to the on-off valves. These considerations are therefore also included and a conceptual design of a bi-directional check-valve is also presented. The structure of the chapter is therefore that the valve design based on the Danfoss Power Solutions PXE-pilot stage is first described along with the results obtained with this valve. This is followed by a comparison and feasibility evaluation of both the on-off valve topology and the bi-directional valve topologies, with regard to a good PTO force control with low energy losses. Finally a conceptual design of the bi-directional check valve is presented along with a conceptual design of an on-off valve based on the same topology as the bi-directional check-valve. This is done based on a theoretical investigation of the pressure switching characteristics, supplemented by simulation models utilised to demonstrate an expected dynamic behaviour of the valve concepts. The chapter concludes with a discussion of the valve configuration in the switching manifold.

3.1 Danfoss Based Valve Design

As described above, no commercial suited valves exist for this kind of switching manifold, and a part of the project has therefore focused on investigating, whether a suited valved could be developed based on the pilot stage (PXE) of a Danfoss Power Solutions PVX-valve, as shown in Fig. 3.1. Based on simulation studies and investigation of the time requirements, power requirements and losses associated with the valve switching, safety requirements and expected lifetime switches, the following requirements were identified:

- The valves should be of the normally closed (NC) type
- Bi-directional flow requirements up to 800 l/min, with a maximum pressure drop of 5 bar
- Working pressure up to 350 bar
- Switch times below 15 ms from signal is enabled - any dead time for the valve should be constant (repeatable), [10]
- Constant switch times (for respectively opening and closing, the two need not be the same) regardless of the operating conditions
- Be able to withstand 1.2 billion cycles
- The valve does not have to be leak proof (minimal leakage is acceptable)

These requirements have been the background for the investigations and design of the prototype valve. The results of this work is summarised in the following. A further elaboration may be found in [22], which includes many of the design considerations and conclusions obtained with the valve.

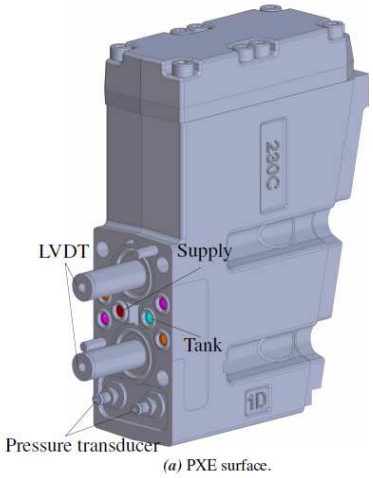

Figure 3.1: Illustration of PVX pilot stage.

3.1.1 PXE-Valve and Modifications

The original PXE is designed with two similar spools, where one is used to control the main spool controlling flow from the supply to the consumer ports (A/B) and the other controls the main spool controlling flow from the consumer ports to tank. In the present design for the on-off valve, the two spools are instead used in parallel to actuate the main spool, hereby increasing the possible flow rate to the valve. This is done, as the transient flow consumption, when actuating/switching the main spool, is much higher for the on-off valve than for the standard PVX-valve. For the same reason the area characteristic of the PXE spool has also been modified, where the overlap has been reduced and the area gradient has been significantly increased, as shown in Fig. 3.2. Practically the modifications to the valve have been implemented by changing the notches in the spools and changing the padding in the housing of the valve.

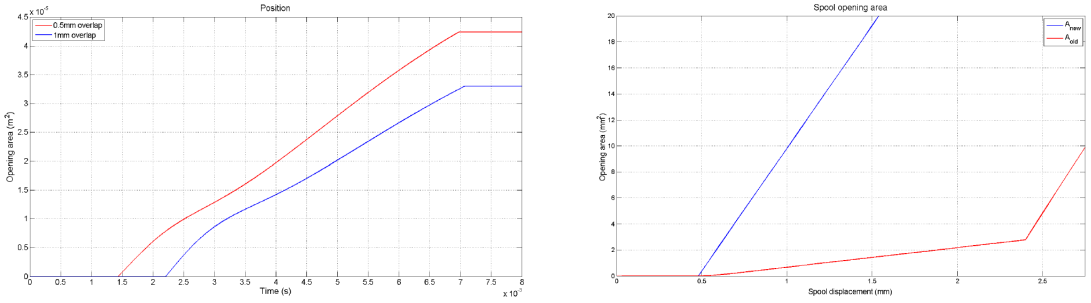

Figure 3.2: Modifications of the original PXE-valve. To the left the time response for decreased overlap and to the right the modified opening characteristic.

The basis for the design of the main stage of the valve is that this is optimised in combination with the PXE valve and its dynamic. As basis for the optimisation a model of the PXE valve was developed, which was also used for the above redesign of the spools and padding, and the model was experimentally verified. The experimental set-up used for the validation of the model is shown in Fig. 3.3.

In the set-up it was chosen only to test the one spool, as the two spools are identical and connected to the

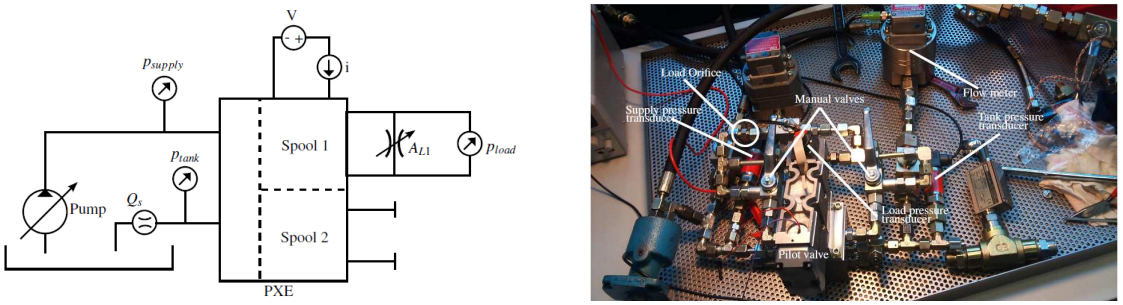

Figure 3.3: Laboratory set-up for validating the PXE-spool characteristics and model. To the left the simplified schematic set-up and to the right a picture of the actual set-up.

same supply internally in the valve. Combined with that there is no position feedback in the valve, it is not possible to ensure that either of the two spools could be slightly biased to one of the side. Hence to avoid dynamic coupling between the two valve when testing, only one of the spools was tested. For the same reason there may be a small leakage flow across the second spool which has not been accounted for. The results of the validation is shown in Fig. 3.4, which shows the flow and pressure drop across the load valve (A_{L1}) , when the system is applied current steps. In the measurement the flow spikes are captured, which is due to the flow meter, which has a limited bandwidth, and other flow meters with both better dynamic capabilities and sufficient accuracy in the measuring range is available.

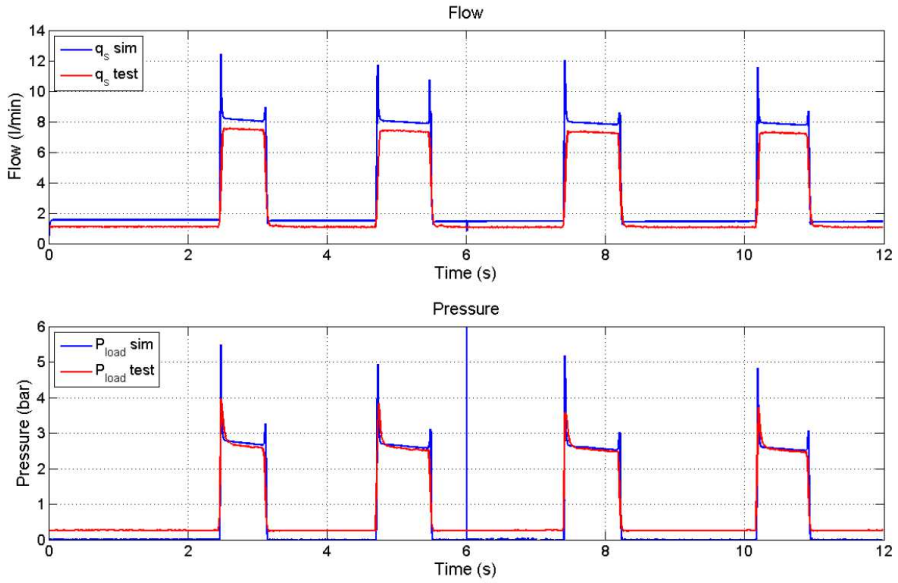

Figure 3.4: Validation of PXE, when applying current steps to the spool.

From the results it is seen that there is good correspondence between the model and the measured flows and pressures. The steady state deviation for the flow is within what could be expected with the present experimental set-up, and although in the high end, it has been considered sufficient for validating the behaviour of the model. The latter should also be seen in relation to the experimental set-up for testing the valve, which has been available at Danfoss Power Solutions. The pressure response is in good agreement with the

measured, also for the dynamic part. For the test set-up the pressure gradients are however more determined by the volumes in the system than the dynamics of the valve, why the experimental results only validates the model, which is then used to determine that the valve dynamics is sufficiently fast for it to be usable as the pilot stage in an on-off valve. The considerations for the valve design are therefore presented next.

3.1.2 Initial Investigations and Conceptual Design

Based on the PXE-valve, the model of this and the valve requirements, a number of different topologies where generated and investigated with regard to both functionality, feasibility, pressure loss, moving mass, actuation requirements etc. Illustration of the different conceptual designs are presented in Fig. 3.5, along with some of the results from one of the preliminary CFD-analysis of the first concepts. From the initial concepts and the analysis of these, a concept was generated, which is essential a spool valve design, based on the concept of a seat valve, but without the seat. The design of the main stage of the valve may be seen in Fig. 3.6, along with indication of the main parts in the valve.

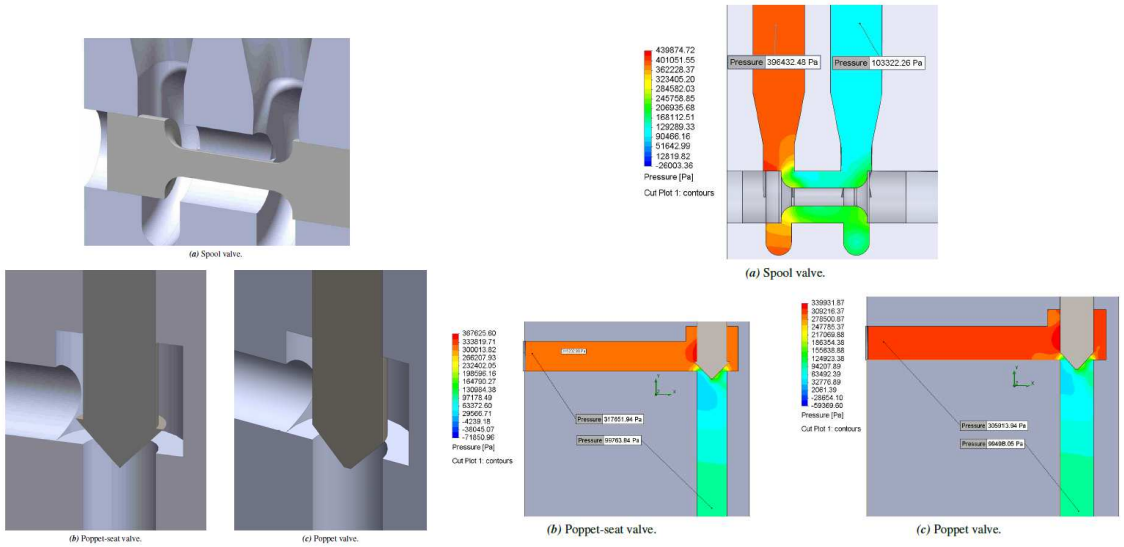

Figure 3.5: Left different concept topologies and right preliminary CFD results for the different concepts.

The final concept emerged from the initial concepts based on the requirement of minimal pressure drop across the valve, where the funnel shaped inlets were optimised based on CFD-analysis of the design to have a smooth flow path and minimal restrictions, see Fig. 3.7. Similarly the requirement for being able to withstand the 1.2 billion opening and closing cycles, directed the solution towards the spool-based principle, where there is no impact, when closing the valve. This principle was based on inspiration from valve designs employed in the manufacturing industry, where they have been tested for up to several hundred million actuations. The downside of this design is a required overlap and hence (limited) leakage flow and an introduced dead time in the design. These limitations where however outweighed by the other design limitations, once it was found that the design specifications regarding leakage flow and switching time could be reached with the developed concept. In the design the spool is hollow to reduce the weight, and the spring chamber is pressure compensated to the a-port to balance the pressure forces. Similarly the pilot actuation chambers and the pilot areas were optimised to suit the PXE-valve, to obtain the best compromise between bandwidth (flow requirements) and still have sufficient actuation forces. The guide attached to the spool and connected

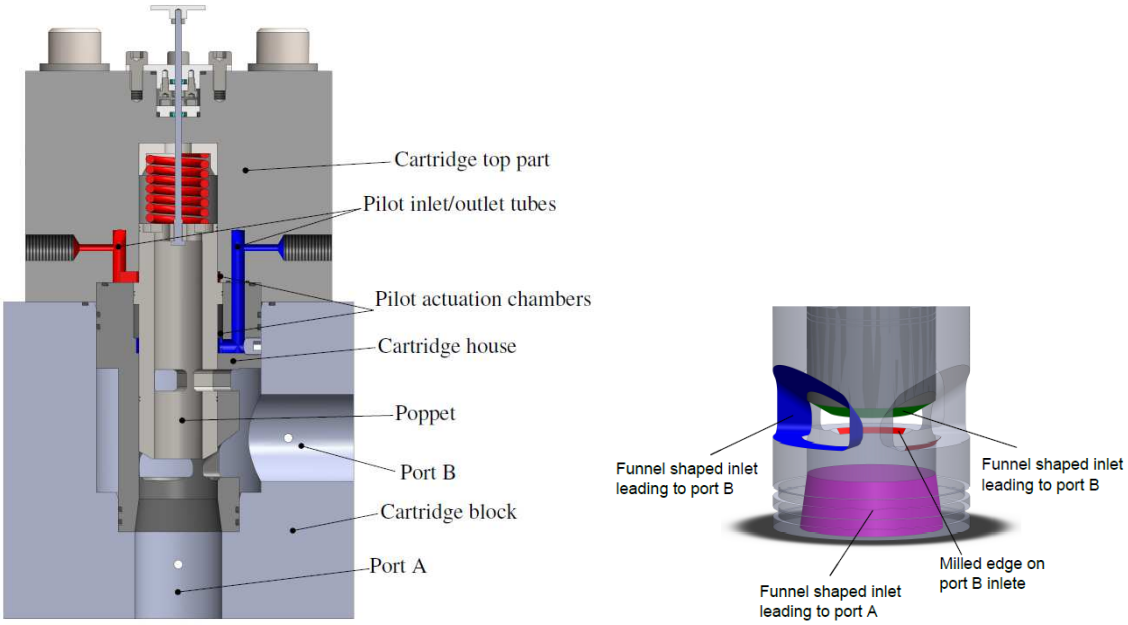

Figure 3.6: Left: a cross sectional view of the final design of the valve, with indication of the main parts in the valve. Right: the design of the poppet and the sleeve (house).

through the spring chamber is included in the prototype to be able to measure the spool position, using a high precision laser beam sensors, where the circular disc in the top the guide is a reflective surface. A sketch of the assembled valve with the position sensor and PXE pilot valve may be seen to the left in Fig. 3.8. The right part of the figure shows the main components of the valve, incl. poppet, cartridge house and block.

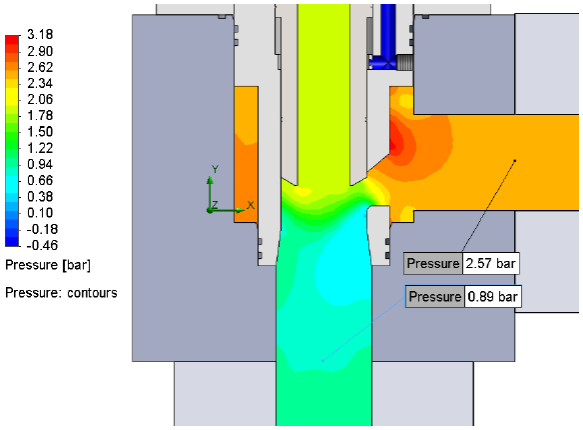

Figure 3.7: CFD-analysis of the final design. The plot shows the pressure distribution in the valve, when specified a flow of 800 l/min.

As part of the valve design, the loading of the mechanical parts is of major importance to accommodate the lifetime requirements. All parts of the valve have therefore been designed for an infinite number of actuations and full range pressure pulsations, where all critical parts have been checked for stress concentrations under

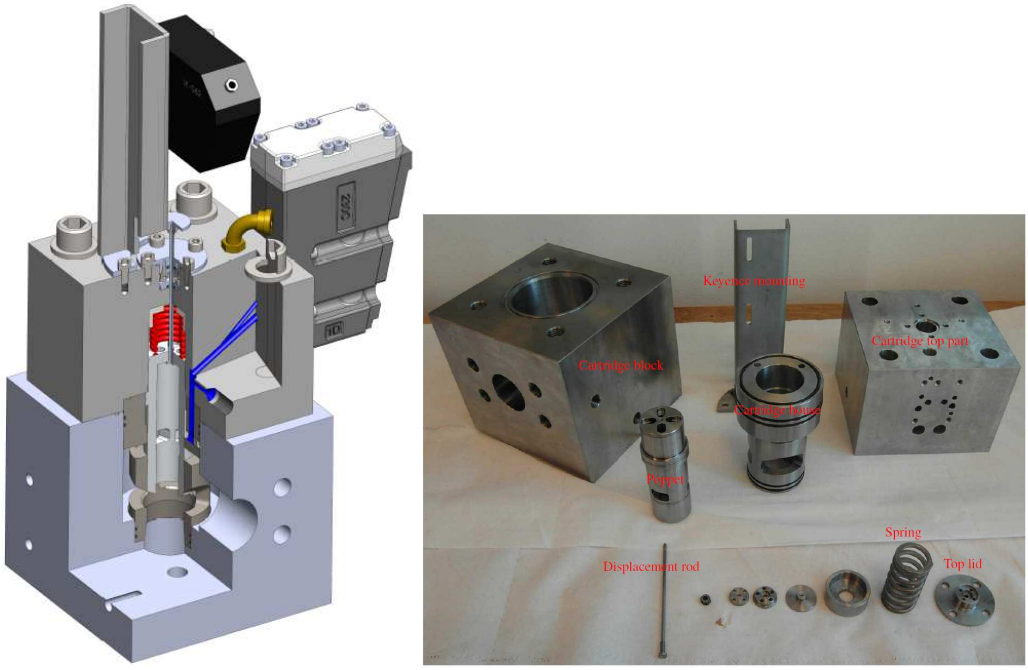

Figure 3.8: Left: cut-trough illustration of the designed valve with PXE-pilot. The top black box is the high precision laser sensor, which measure the main spool position. The blue shaded area is one of the pilot supplies from the PXE to the main valve. Right: the main components of the manufactured prototype valve.

worst case operating conditions. As an example the stress distribution for the poppet is shown in Fig. 3.9. To accommodate the infinite lifetime all parts have been made using steel alloys. The design has furthermore been made based on normal valve design considerations concerning leakage, manufacturing tolerances, etc. Based on the developed design a prototype was manufactured and tested. The results from these tests are presented next.

3.1.3 Experimental Testing and Results

For testing the prototype valve, the experimental set-up illustrated in Fig. 3.10 has been used. Ideally the valve should also have been tested in the test bench described in chapter 4. However, based on the below findings and delays with the test bench set-up, this has been abandoned. Instead both static and dynamic tests have been performed with the below set-up.

In the test the system is run with near constant supply and pilot pressure (pressure level could be adjusted). The back pressure (measured at port 2) for the valve is then adjusted using the variable orifice, whereby the pressure drop across the valve may be adjusted (statically). The accumulator on the pilot line is included to reduce pressure variations on the pilot line. During the tests both differential pressure and absolute pressures are measured, as the differential pressure transducer has a limited measuring range. Similarly the flow sensor used to measure the main flow is limited to 150 l/min, why the measurements have been limited to this value. Practically the tests have been performed as both static tests, measuring the $p-Q$ characteristic for the valve and dynamic tests, where the opening characteristics, pressures and flows have been measured. The result of the static test is shown in Fig. 3.11, which shows the pressure drop for the valve for different flow rates and

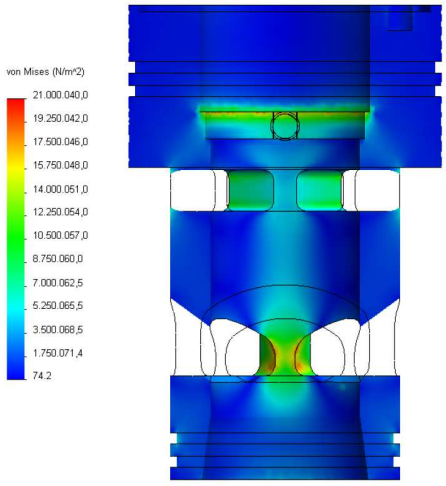

Figure 3.9: Stress in the poppet for worst case operating conditions, i.e. when the poppet hits end stop with maximum velocity under full pressure.

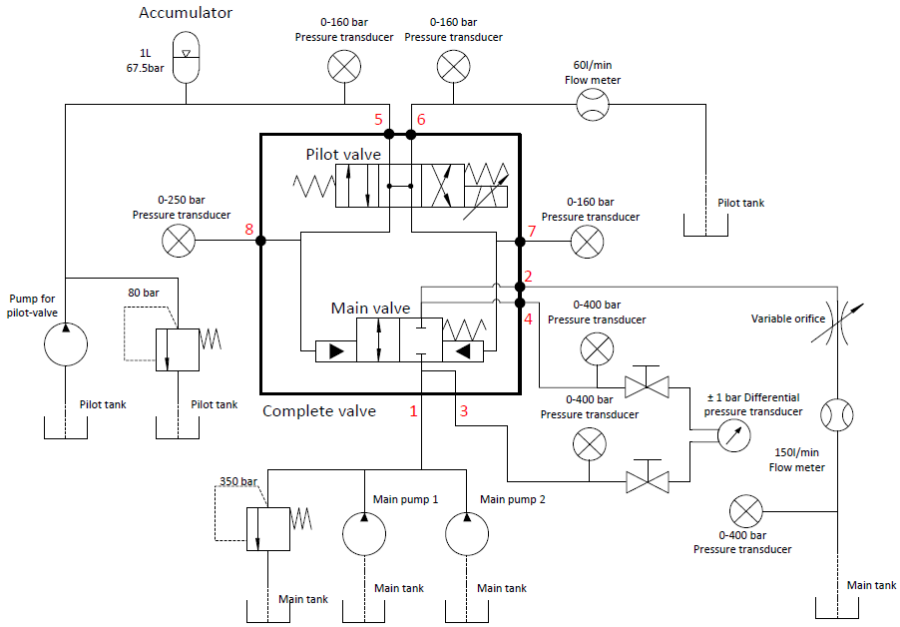

Figure 3.10: Diagram for the experimental set-up for testing the valve. The HPU-part is simplified.

for a fully open valve.

From the results in the figure it is seen that there is very good correspondence between the measured and calculated pressure drop across the valve, especially considering the very low pressure drops. The measures pressure drop is here actually slightly lower than the calculated pressure drop, but the deviations are within the measurement accuracy of the differential pressure transducer. Due to the limitations of the flow sensor it has not been possible to measure at higher flow rates, but based on the correspondence between the measured

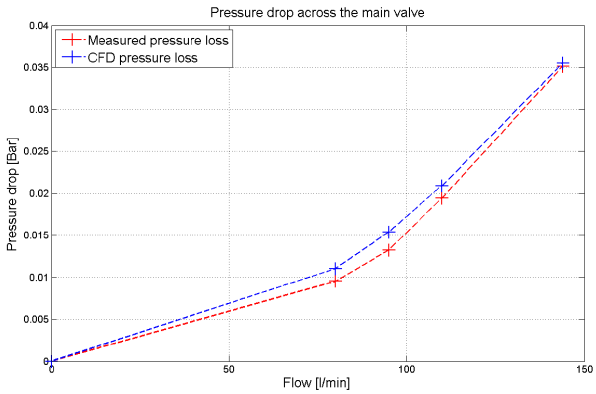

Figure 3.11: Static verification of pressure drop for the valve

and calculated pressure drops, the model is considered valid. Hence, based on the CFD-model it is found that the pressure drop in both directions is below 1.5 bar for a full flow of 800 l/min, and the valve therefore statically fulfils the flow requirements.

Dynamically the valve is also able to open and close within the specified requirements as shown in Fig. 3.12 for the opening situation. The opening situation is here the most critical, as the flow forces here will tend to close the valve.

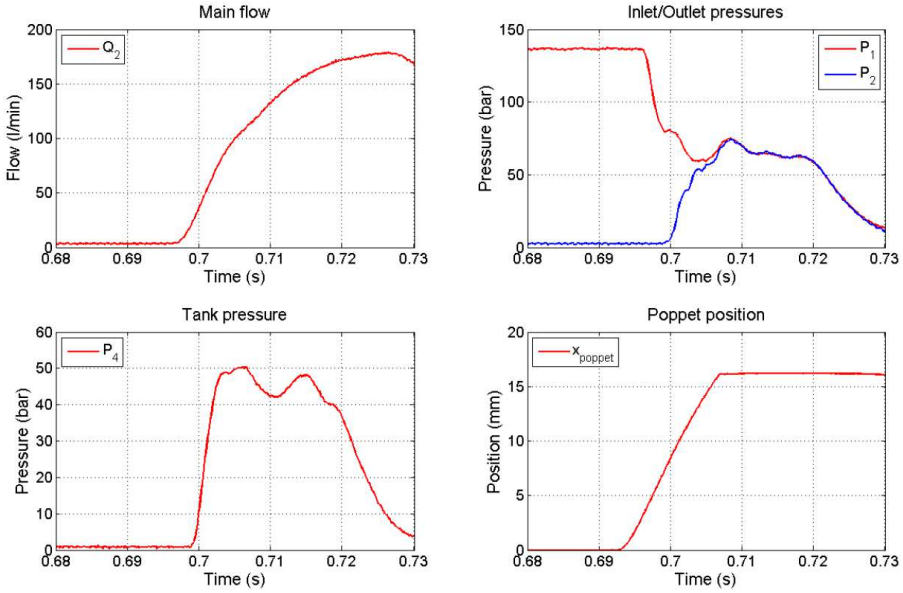

Figure 3.12: Measured flow, pressures and poppet position, when applying a 2 A current step.

From the figure it is seen that when the valve starts opening the main flow increases and the pressure difference across $(p_1 - p_2)$ the valve drops to below 1 bar, whereas the tank pressure dynamically rises to almost 50 bar. It should in this regard be noted that part of the dynamics in the response is due to the dynamics in the hydraulic power unit and the long return lines to tank. From the figure it may furthermore be seen that after the valve has been open the pressures decreases to about 15 bar, which is determined by the setting of

the variable orifice for the given flow rate. It should furthermore be noted that the flow dynamically exceeds the limitations of the flow transducer and the results above 150 l/min should therefore be taken with some caution as this is outside the specified measuring range for the flow sensor.

Considering the valve behaviour, this is also in fairly good agreement with the model predicted behaviour, as may be seen from Fig. 3.13, which shows the measured and simulated poppet position, main pressures, differential pressure and the actuation pressure, i.e. pressure across the PXE. From the figure it is seen that the model captures the characteristic behaviour of the valve and the pressure dynamics. In reality the model is however very sensitive to the end position viscous friction in the model, i.e. the suction effect that arise, when the contact surfaces (in the pilot actuation chamber) of the main spool and the cartridge separates. This is so even though the contact surfaces have been minimised and lubrication paths have been introduced in the design.

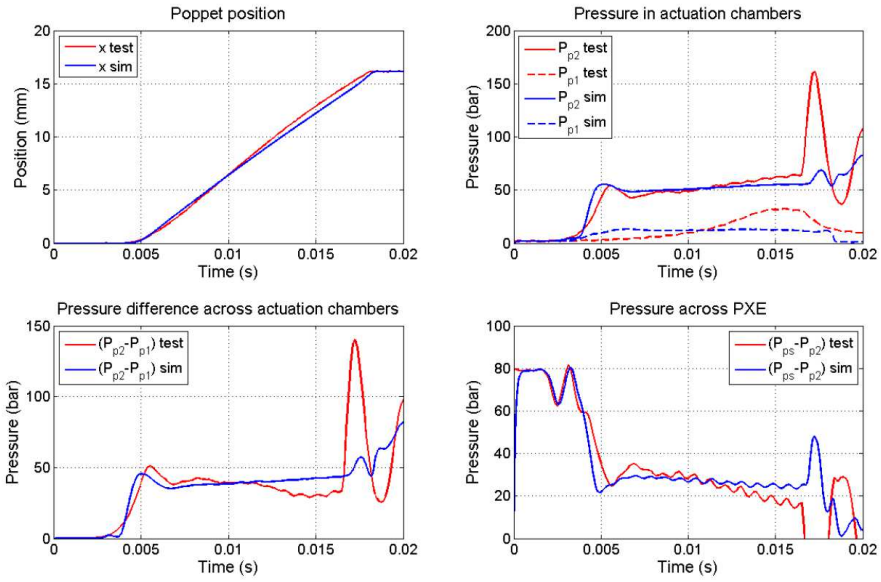

Figure 3.13: Measured poppet position and pressures, when applying a 2 A current step.

One of the problems with the prototype valve is that the PXE pilot stage utilises both the two spools to supply sufficient flow to the main stage, and that these two spools are controlled open loop, by just giving the same signal to the two valves. During the opening and closing of the main stage, this is a minor problem, but when the main poppet is to be kept in a given position and/or if applying artificial end damping this is a problem as one valve may essential be open to tank, while the other is open to supply or vice versa. I.e in zero position the two spools are ideally in the centre position, but in practice they are both biased and the bias is unknown. This may have several implications as an increased power consumption due to a short circuit flow across the pilot stage and possible increased dead time for the main stage, as the pilot spools have to travel further before the valve starts opening. The latter may generally be considered a reduced controllability of the valve, which is a problem, as the bias of the spools decreases the repeatability for the valve. Hence combined with the end friction (suction) phenomena, it is not possible to e.g. introduce open loop end damping for the main stage based on mapped performance of the valve. In practice the problem of bias of the pilot spools was, however, of limited influence for the produced prototype valve, where the opening and closing times were consistent for the tests performed.

3.1.4 Conclusions for PXE-based Valve

Based on the developed prototype and the experimental testing of this. A number of conclusions were reached:

- Due to limitations in the test set-up, it was not possible to test the valve with the maximum flow of up to 800 l/min. The maximum flow rate tests were carried out at flow rates[1] of 170 l/min, but based on the results and the very good correspondence with the models it was assessed that the valve will have no problems in handling the maximum flow and within the specified pressure drop across the valve.
- Structural FEM analysis verified that the valve is capable to operate with pressures up to 350 bar with more than 20 years of operation
- Experimentally validated CFD-analysis showed that the valve has a pressure drop below 1.5 bar for a flow of 800 l/min in both directions
- The valve opening and closing times are fairly constant at 15 ms and 13.5 ms respectively, of which the dead time is approx. 2.3 ms
- The leakage flow for the valve is measured to approx. 2 l/min for a working pressure of 200 bar

Overall the valve therefore fulfils the design specifications, and the next step would be to test the valve in the switching manifold on the test set-up described in chapter 4. In reality there are, however, a number of factors that may influence the feasibility of the design. Firstly the experimental testing revealed that the impact when the spool hit the end positions was significant and this introduced pressure spikes in the test set-up, and although the valve was designed for these impact forces (stress wise) and does include some hydro-mechanical end damping, the possibility for surface fatigue (wear) have to be looked further into. The latter is also the case, as it was also expected that some artificial damping should have been implemented via the control to reduce the impact forces. However the problem with using two spool valves limits this possibility. Secondly the valve design was based on the modified PXE-valve, which both require extra manufacturing, but which is either not intended for this purpose, and hence is designed for a much lower number of actuations in the lifetime. Combined with the development and testing of the Bucher valve and the other valves described next, the further development of the valve design based on the PXE-pilot stage was therefore stopped until the prototype could be first tested on the full scale laboratory set-up.

3.2 Analysis of Valve Topology

The original concept for the switching manifold was based on using on/off valves to directly control which pressure line is connected to each of the cylinder chambers. This will imposed a PTO force continuously controlled by the valve settings. However, the inevitable energy loss due to the pressure shifts and the timing issues in valve actuation posses a problem, which may potentially be reduced by using bidirectional check valves. A bidirectional check valve (BCV) is in this connection a valve configuration working as a spring loaded check valve for which the checking direction may be changed. Due to the possibility to overcome some of the problems with using on/off valves, the study has been broadened to also consider BCVs as

[1] The maximum measured flow rate. The flow meter is only specified to 150 l/min, but did still provide reasonable data up to 170 l/min, although the maximum flow rate should be taken with some uncertainty.

oppose to on/off valves in the switching manifold. In the following the results of this feasibility study and comparison with on/off valves are presented. This is done firstly for a general discrete force system and afterwards directly when related to a discrete force system designed for WECs.

The analysis is made for the case where the valves are designed with equal nominal pressure drop at nominal piston velocity, hence, the flow rate for each valve fits the cylinder chamber to which it is connected. The on/off valves are in the topology analysis modelled as simple 2/2 valves. The bidirectional check valves are on the other hand modelled as ideal spring loaded check valves, for which the flow direction may be changed. The opening area is for both valves types modelled linearly proportional to the valve poppet position and the valve flow is modelled utilising the orifice equation [18]. The dynamics of both the on/off and BC valves are modelled ideally, hence the on/off valve switches states infinitely fast and force balance is always present for the BCV poppet.

The pressures in the cylinder chambers are in the proposed discrete fluid power force system controlled by the pressure line to which each chamber is connected. However, during connection shifts varying pressure dynamics may be experienced in the cylinder chamber, e.i. the pressure gradient is determined based on whether the cylinder is extending or retracting.

The application of the discrete force system entails the loading on the force system. Hence, if the force system is utilised to actuate a system with a low inertia and driving force, the force from the cylinder chamber pressures may easily overcome the load and inertia and entail the system movement. On the other hand, a system with large inertia and large driving force (as for the Wavestar float arm) may be able to overcome the force from the cylinder pressures. This way the fluid force is only opposing the movement enforced by the load. Hence, the kinetic energy of the float and the force applied on the float is sufficient to induce a pressure build-up in the cylinder chamber. In the weak loaded system where the load do not carry enough energy to induce a pressure build-up, a pressure change from one pressure line to another may only be accomplish by switching the valves. However, for a system with a load force exceeding the fluid force from the discrete system, a pressure change may be accomplished by closing all valves and using the driving load force to enforce the compression or decompression required to yield a pressure change. Hence, the bidirectional check valves are not feasible in systems where the discrete force system is the driving system. In wave energy converters the PTO-system the opposite is however the circumstance, i.e. the WEC is the driving force and bidirectional check valves may be feasible alternative to on/off valves.

The feasibility of bidirectional check valves is analysed by comparing BCVs to on/off valves, in paper [E]. The two valve types are compared by time simulations of a single float Wavestar WEC model utilising the on/off and bidirectional check valves respectively. The comparison is carried out with two system configurations (given later) in terms of the multi-chamber cylinder and the common pressure lines. The valves are evaluated on the energy output to the common pressure lines, the system behaviour and the structural loading imposed.

3.2.1 Pressure dynamics

The pressure dynamics in the multi-chamber cylinder will be affected by using bidirectional check valves compared to using on/off valves. Furthermore the pressure in the cylinder chambers are highly affected by the switching time of the valves and the timing between disconnecting from one pressure line until connecting to another pressure line. The pressure dynamics is both depending on the displacement of the piston and the valve flow into or out of the cylinder chamber. The hydraulic capacitance, given by chamber volume and oil stiffness, furthermore entails the pressure gradient at a given difference in volume change and oil

inflow. This is explained in the following, where in Fig. 3.14 a force shift is illustrated, while the piston has a negative velocity. In chamber 1 a pressure shift from line 3 to 1 is made by disconnecting from line 3 and letting the piston moment impose a pressure decrease by increasing the chamber volume, while connecting to line 1 when the chamber pressure gets just below line pressure 1. On the other hand the pressure decrease in chamber 2 from line pressure 3 to 2 is accomplished by actively disconnecting from line 3 and in same instant connecting to line 2, hence the pressure decrease is accomplished by the flow out of the chamber across the valve.

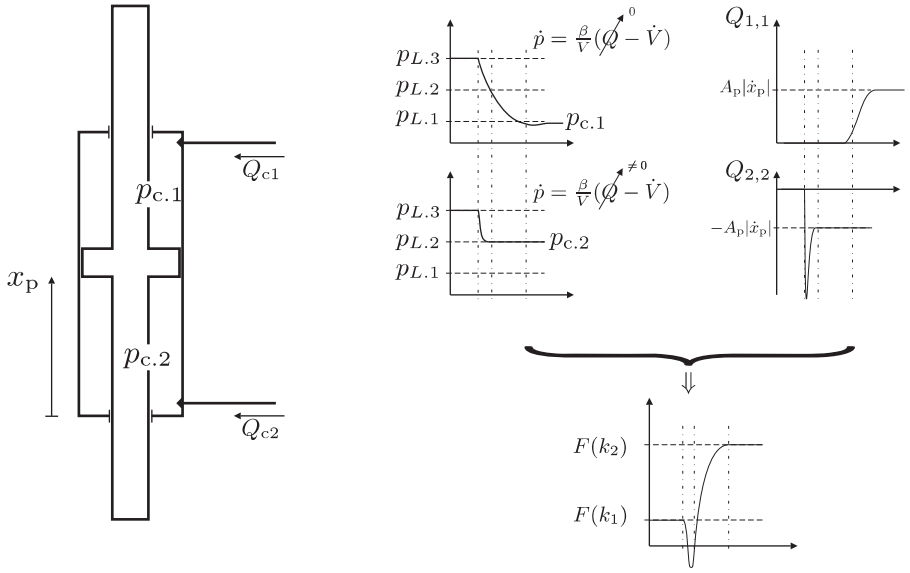

Figure 3.14: Illustration of chamber pressure dynamics and resulting cylinder force.

It is seen in Fig. 3.14 how the two type of pressure shifts impose significant different pressure dynamics in the cylinder chambers. Further it is seen how the valve flow differ with the active valve leading to a significant flow peak yielding a high energy loss. Lastly the resulting force is illustrated, from which one should note that the large difference in pressure gradients impose an unwanted force peak.

The large flow peaks due to the connection of a cylinder chamber at a given pressure to a pressure line with significantly different pressure will enforce energy losses due to throttling. The force peaks may result in poor PTO force tracking hereby degrading the energy extraction from the ocean waves. While this may decrease the energy production, the force peaks may also impose and increase structural loads on the float arm.

3.2.2 Comparison of Valve Topology

The extracted energy, the energy output to the common pressure lines and the dynamic performance of system utilising on/off or BC valves are investigated in paper [E]. The investigations are conducted for the two system configurations seen in Fig. 3.15. System 1 consist of a symmetric two chamber cylinder in connection with four common pressure lines, whereas System 2 consist of a three chamber cylinder and three common pressure lines. The valve connection is here illustrated as two check valves, indicating the function of the BC-valve working as a check valve in either direction based on the pilot settings.

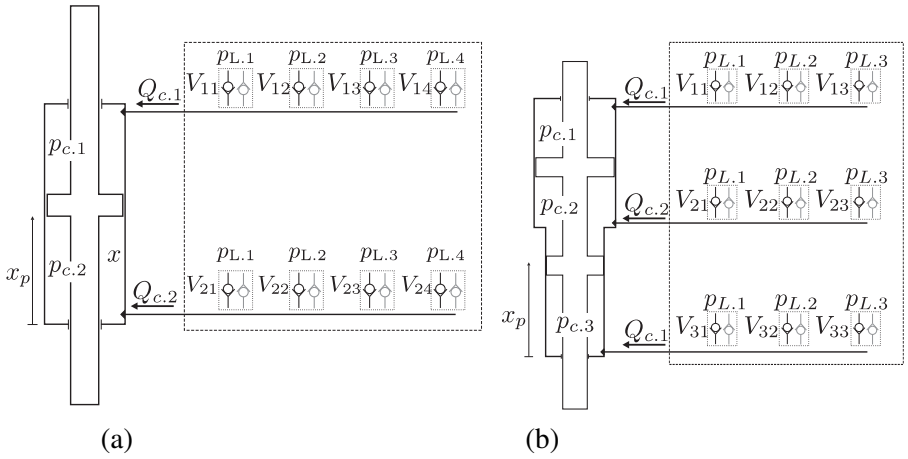

Figure 3.15: Illustration of the system configuration utilised in the feasibility study of BC valves. System 1 (a) and System 2(b).

The extracted energy and the energy output to the common pressure lines are close to equal for the system utilising on/off and BC valves, however the conversion efficiency is seen to be slightly higher for the BCV system. Hence, a smaller energy loss is obtained in the system. On the other hand the amount of extracted energy is higher for the on/off valve system due to a better force tracking. An example of the energy results are given in Fig. 3.16. Note the very small difference in the average power obtained.

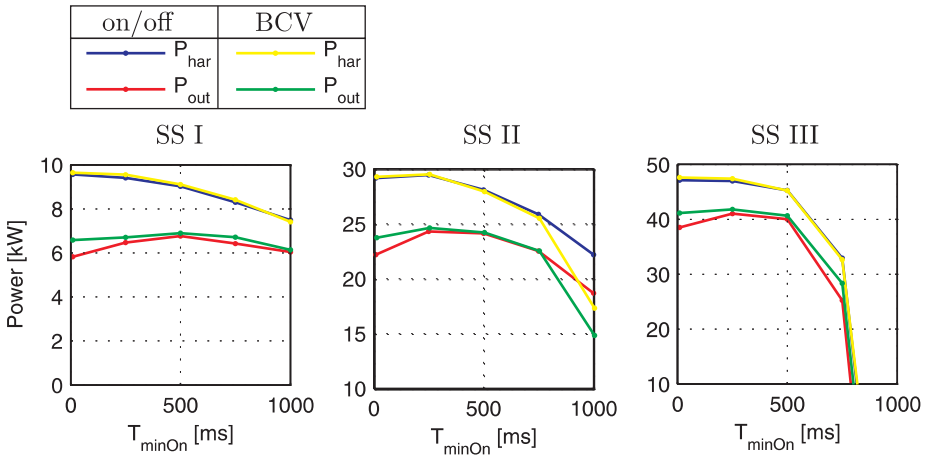

Figure 3.16: Average harvested power and power output for systems utilising on/off and bidirectional check valves respectively. The results are given for the three sea states.

The bidirectional check valves impose some pressure shifts with huge difference in pressure gradients yielding a large number of unwanted force peaks. These extra force peaks may lead to fatigue problems due to the added number of loads and the increased loads. To evaluate this extra loading on the mechanical structure of the WEC the force steps imposed are counted and arranged in intervals. Figure 3.17 shows the number of force steps in each interval for the discrete force reference (blue bars) and the number of actual applied force steps (black bars) utilising on/off and BC valves respectively in combination with System 2.

The actual applied force is clearly seen to be shifted to the right for the BCV system, hence larger force steps

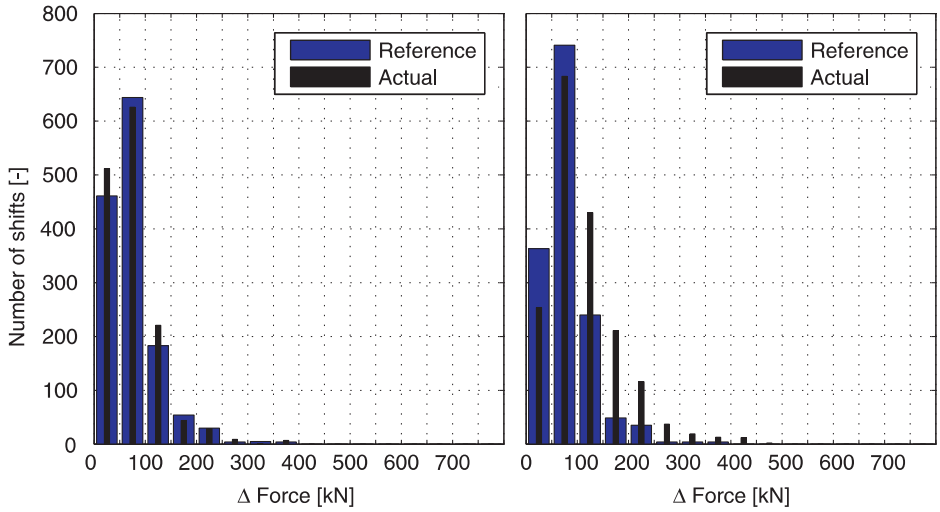

(a) (b)

Figure 3.17: Force shifts counts for system 2 utilising on/off and bidirectional check valves left and right respectively.

are imposed than indicated by the reference. For the on/off valve system on the other hand the actual force steps are rather close to those of the force reference. Similar results are obtained when employing system configuration 1, though the force shifts imposed are larger.

The topology analysis demonstrates that bidirectional check valves and on/off valves imposes approximately equal energy output, however the use of bidirectional check valves yield some minor increase in the structural loads applied to the float arm from the multi-chamber cylinder. The conclusion is therefore that from a conceptual point of view bidirectional check valves are feasible for use in the wave energy converters, however they do not necessarily yield better results than using on/off valves, but this is highly linked to the design criteria of the WEC, the control of the PTO-system and the realisation of the valves, which is discussed next.

3.3 Conceptual Design of Valve for Switching Manifold

The above analysis show that conceptually BCVs may be a feasible alternative to on-off valves, hereby possibly overcoming some of the timing considerations for the switching. However, to take the analysis a step further the limitations in actually realising the valves have to be considered. In this section the conceptual design of the valves for the switching manifold is therefore considered. This is done for both a conceptual BCV, but also for a similar type on/off valve (based on the same design ideas), to be able to compare the results. The valve designs considered in this section should therefore be seen as complementary to the initial investigated valve design based on the PXE pilot stage, where some of the problems with the pilot stage may also be overcome.

Both the two valve types considered in this section are designed as two stage piloted valves, where both the main stage, the pilot stage and the combination of the two stages are discussed. A major issue is the configuration of the pilot system since this entails the functionalities obtainable and some practical requirements for the manifold design. In Fig. 3.18 various set-ups of the pilot system are illustrated.

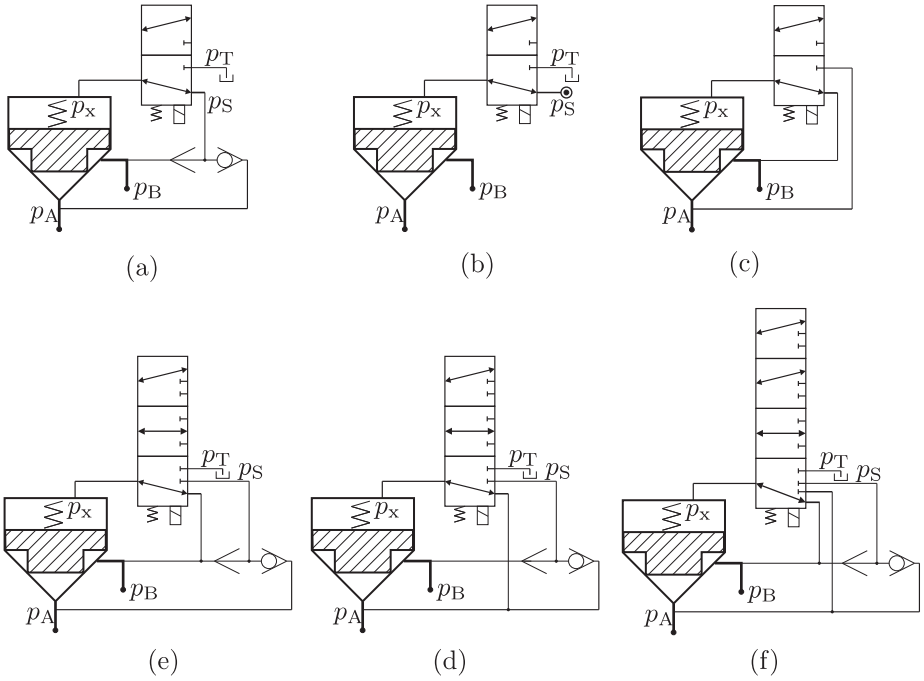

Figure 3.18: Illustrations of conceptual pilot system configurations.

Some concepts; (b) and (c) are fully electronic controlled, whereas concepts (a), (d), (e) and (f) are partly hydro-mechanically controlled. The shuttle valve included in (a), (d), (e) and (f) induces a stay closed stage, and hence, the requirements for the pilot valve may be lowered. The functionality of the six valve concepts in Fig. 3.18 are briefly described in the following:

(a) This valve concept is an on/off valve. The pilot pressure p_x may either be set to tank pressure or the highest valve port pressure, leading to a valve having two states. Closed or opened, for the pilot pressure equal to highest port pressure and tank pressure respectively. This concept requires an external tank connection and a shuttle valve.

(b) This valve concept is an on/off valve. The pilot pressure p_x may either be set to tank pressure or pilot supply pressure, leading to a valve having two states. Closed or opened, for the pilot pressure equal to pilot supply port pressure and tank pressure respectively. This concept requires an external tank and supply line. Furthermore, the pilot supply pressure must be higher than the highest pressure at the valve ports at any time.

(c) This valve concept may be utilised both as an on/off valve and a bidirectional check valve. The pilot pressure p_x may be set to either of the port pressures p_A or p_B, leading to a valve having two states. However, which of the pilot settings that leads to an open or closed main stage is dependent on the sign of the port pressure difference defined as $\Delta p = p_A - p_B$. Hence, this valve concept do not require any external connection, but pressure measurements are required when choosing pilot valve position based on opened or closed signal. This valve concept works as a check valve with flow from A to B by letting $p_x = p_B$ and vice versa for opposite flow direction.

(d, e) These concepts are one directional check valves with forced on/off valve possibility. The pilot

pressure p_x may either be set to tank pressure, the highest valve port pressure or the port pressure at A or B for (d) or (e) respectively, leading to three states for the valve control. The first two gives opened and closed states and the third gives checking possibility in one direction. (d) checking from port B to A and (e) checking from A to B, this third stage make little sense when the area configuration is made as on/off valve. This concept requires an external tank connection and a shuttle valve.

(f) This valve concept is primarily a bidirectional check valve with forced on/off possibility. The pilot pressure p_x may either be set to tank pressure, the highest valve port pressure or either of the two port pressures p_A or p_B, leading to opened or closed stage for pilot pressure equal to highest port pressure and tank pressure respectively and checking in each direction depending on the connected port pressure. This valve requires an external tank connection and a shuttle valve.

3.3.1 Main stage topology

The main stage of the switching valve is in this conceptual design considered for a rated flow of 1000 L/min@5bar and to allow fast valve switching, i.e. less than 15 ms. Two poppet topologies are investigated as illustrated in Fig. 3.19. Both valves have main flow path between p_1 and p_2. The pilot pressure, p_x may be set to either tank pressure, p_T and the pressure at port 1, p_1. Hence, the valves given in Fig. 3.19 are similar to the valve concept in Fig. 3.18 (a), though, the shuttle valve is omitted and only port A/1 may be utilised. However, with some minor adjustments the illustrated valve may be equal to that in Fig. 3.18. In the valves given here the pilot valve is build into the valve housing enabling a compact valve design.

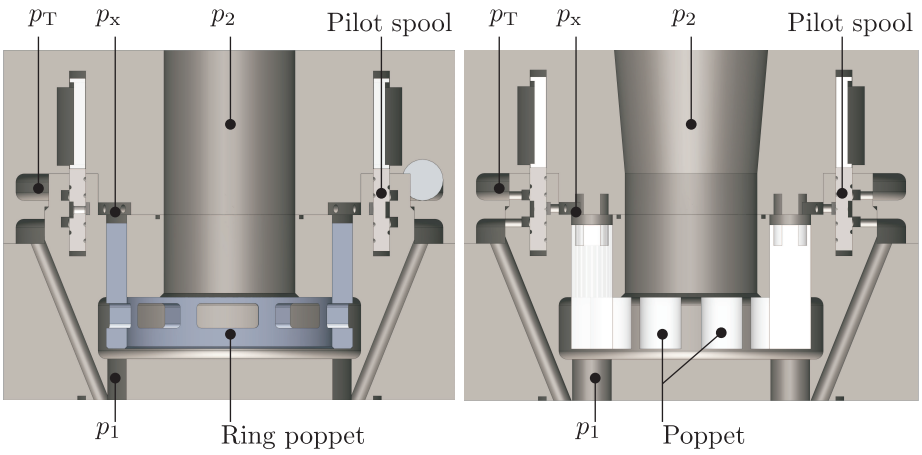

Figure 3.19: Illustration of the two poppet topologies proposed for the main stage. (a) Ring-poppet. (b) Multi-poppet.

The ring-poppet topology (a) utilises a single poppet shaped as a ring. The ring shape is proposed to decrease the poppet mass and the pilot volume compared to a traditional solid poppet. The multi-poppet topology (b) utilises a multiple number of solid poppets. The multiple numbers of poppets requires smaller poppets leading to shorter stroke length and thereby smaller pilot volume. The two poppet topologies are further illustrated in the Fig. 3.20.

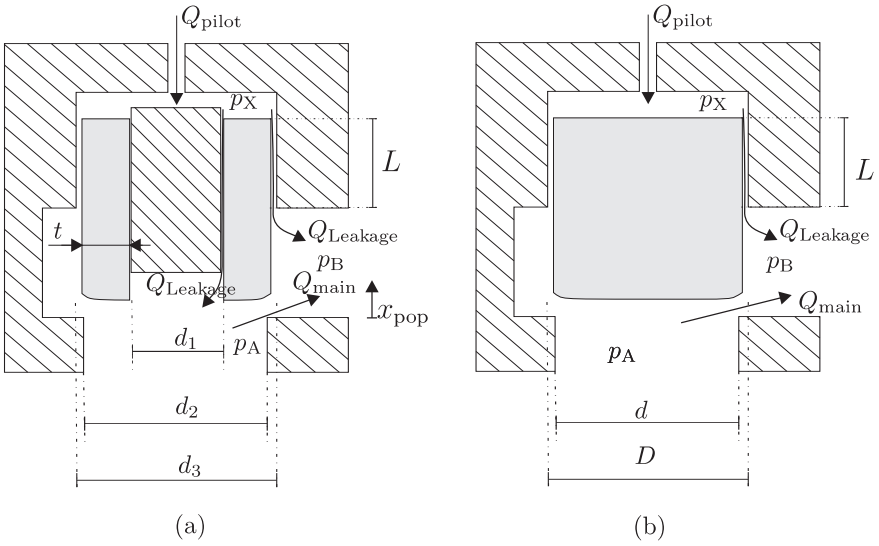

Figure 3.20: Illustration of main stage topologies, (a) ring-poppet (b) multi-poppet.

Design functions describing the poppet diameter, the average needed pilot flow for a full valve stroke and expected leakage flow are derived in paper [F] and [G] for the bidirectional check and on/off valve respectively, and reprinted here for the BC-valve for both the ring- and multi-poppet topology. The functions are based on the nomenclature given in Fig. 3.20.

Multi-poppet	Ring-poppet
$d = \sqrt{\frac{1}{n}} \left(\frac{Q_{\text{nom}}}{C_{\text{d}} \frac{\pi}{4} \sqrt{\frac{2}{\rho} \Delta p_{\text{nom}}}} \right)^{\frac{1}{2}}$ $D = \sqrt{2} d$	$d_1 = -t + \sqrt{d_2^2 - t^2}$ $d_2 = \left(\frac{Q_{\text{nom}}}{C_d \frac{\pi}{4} \sqrt{\frac{2}{\rho} \Delta p_{\text{nom}}}} \right)^{\frac{1}{2}}$ $d_3 = t + \sqrt{d_2^2 - t^2}$
$\Delta V_{\text{X}} = n \frac{d^3 \pi}{8}$	$\Delta V_{ring} = t d_2 \frac{\pi}{4} \sqrt{d_2^2 - t^2}$
$Q_{\text{pilot}} = n \frac{d^3 \pi}{8 T_{\text{sw}}}$	$Q_{\text{pilot.ring}} = t d_2 \frac{\pi}{T_{\text{sw}} 4} \sqrt{d_2^2 - t^2}$
$Q_{\text{leakage}} = n d \sqrt{2} \frac{\pi \varepsilon^3}{12 \mu L} \Delta p_{\text{x-B}}$	$Q_{\text{leakage.ringA}} = d_1 \frac{\pi \varepsilon^3}{12 \mu L} \Delta p_{\text{x-A}}$ $Q_{\text{leakage.ringB}} = d_3 \frac{\pi \varepsilon^3}{12 \mu L} \Delta p_{\text{x-B}}$

Table 3.1: Design function for the bidirectional check valve.

The results of the design functions for the bidirectional check and the on/off valve are seen to be similar for the two main stage topologies. In Fig. 3.21 the needed pilot flow, expected leakage and the poppet diameters are given for the ring- and multi-poppet topology in (a) and (b) respectively, for the bidirectional check valve design.

From the design functions in Fig. 3.21 it is seen that the multi-poppet topology requires less pilot flow when the ring thickness exceeds a reasonable 5 mm and the multi-poppet number exceeds 8. This is seen true

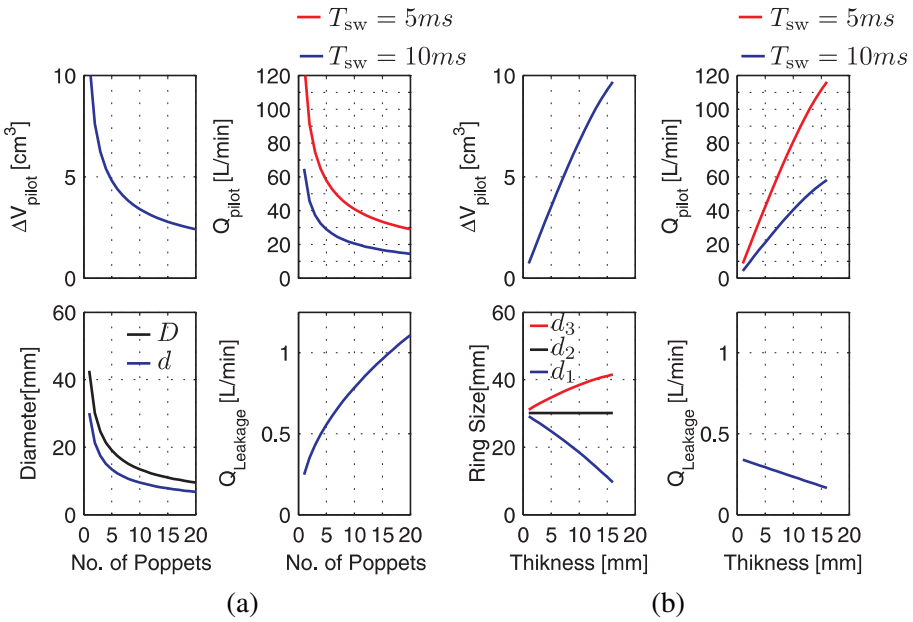

Figure 3.21: Average pilot flow requirements, expected leakage flow and poppet diameter as a function of ring thickness and number of poppets respectively (a) and (b).

for the on/off valve at ring thickness of 5 mm and only 3 multiple poppets in paper [G]. Due to this, the multi-poppet topology is chosen for further studies. However the increase in poppet numbers is followed by an increasing leakage and increasing complexity in the geometric placement of poppets and pilot system.

3.3.2 Pilot Valve

Design of the pilot valve has not been included in the current work, however some various issues concerning the pilot valve have been discussed. In the simulation studies of valve configurations three pilot valves are utilised. The pilot valves included in the simulation models are all state of the art valves. The pilot valves are all 3/2 way valves, the possibility of employing two 2/2 way valves are not included in the simulation model, however shortly mentioned in paper [F] and [G]. Furthermore, special dynamic requirements on the pilot valves for the stay closed state of the bidirectional check valve, 3.18 (c), are discussed in paper [F]. The investigations showed that for on/off valves the rated flow is of great importance. This is also the cased for the BC-valve, however, the BC-valve further requires a fast pilot valve switching if the BC-valve is to be used at intermediate pressure line. In the following section test results from a BC-valve concept test are given. For the BC-valve the pilot valve switching time must be in the range of 2 ms, to avoid unintended opening of the check valve. The required rated flow is found to be highly dependent on the main stage design, however the expected required rated flow is in the range of 20 - 40 L/min@5bar.

3.3.3 Test of Bidirectional Check Valve Concept

The simplest concept proposed for the BC-valve is the one in Fig. 3.18 (b) where a logic main stage with area configuration A:B:X = 1:1:2 is utilised combined with a direct actuated 3/2 valve. The test set-up in Fig. 3.22 was constructed to test the proposed BC-valve concept. A commercial WL22SDxx (size 10 -

125L/min@5bar) Bucher valve was employed as main stage while a FSVi 2.0 (10L/min@5bar) valve from LCM was utilised as pilot valve.

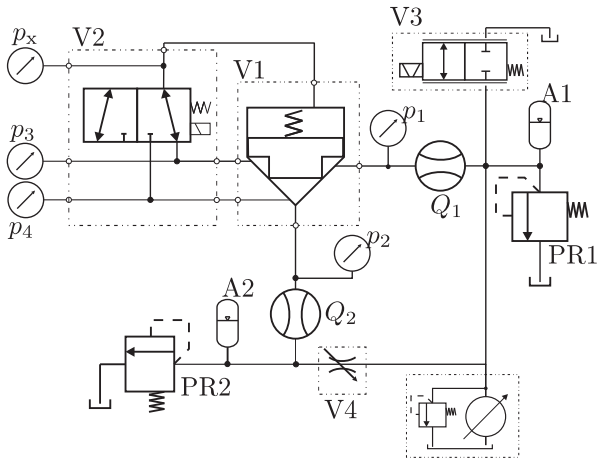

Figure 3.22: Functionality test set-up for the bidirectional check valve concept. V1 is the main stage and V2 is the pilot stage.

With the test set-up the proposed BC-valve concept was shown achievable. In Fig. 3.23 pressure and flow measurements are given for passive and active valve switching as well as for the stay closed mode. All plots in the figure follows the same colour code and shows the same data in the same plot position. Colour code: p_1-red, p_2-blue, p_x-black, Q_1-green, Q_2-magenta, u_{v3}-dash dot blue, u_{v2}-dash dot black.

From Fig. 3.23 the BC-valve concept proposed is seen to work as intended. However, the used test set-up did not allow for a measurements of the valve switching time, which have to be proven in a later design phase.

3.3.4 Simulation of on/off Valve

To facilitate an evaluation of various valve configurations, in terms of number of poppets, choice of pilot valve and pilot pressure configuration, a simulation model has been constructed. The system modelled is illustrated in Fig. 3.24. The valve configuration is directly connected to a cylinder chamber, which is utilised to emulate the volume chamber experienced in the multi-chamber cylinder. The other valve port is connected to a fixed volume with a constant pressure through a fixed orifice. As seen the pilot valve may be connected to either tank pressure, p_T or to the pilot supply pressure, p_S. The pilot supply pressure is either the highest internal pressure, hence, $p_X = \max(p_A, p_B)$ or the pilot supply given as an external supply pressure $p_X = p_{ex}$.

The valve model is constructed in a generic way to facilitate comparison of various valve configurations. Hence, the number of main stage poppets, size and dynamics of pilot valve, spring setting and operating conditions are changeable. The model utilises the orifice equation to model the flow through the main and pilot stage. Several simulation results are given in papers [F], [G] and [H] for various combinations of pilot valve data, number of poppets and system pressure. From the simulations the valve parameters in Tab. 3.2 are found for the on/off multi-poppet valve design, as the best possible compromise.

Simulated poppet position and velocity for the multi-poppet valve with the parameters given in Tab. 3.2 are shown in Fig. 3.25 for the opening and closing of the valve. The results are for three system pressure levels

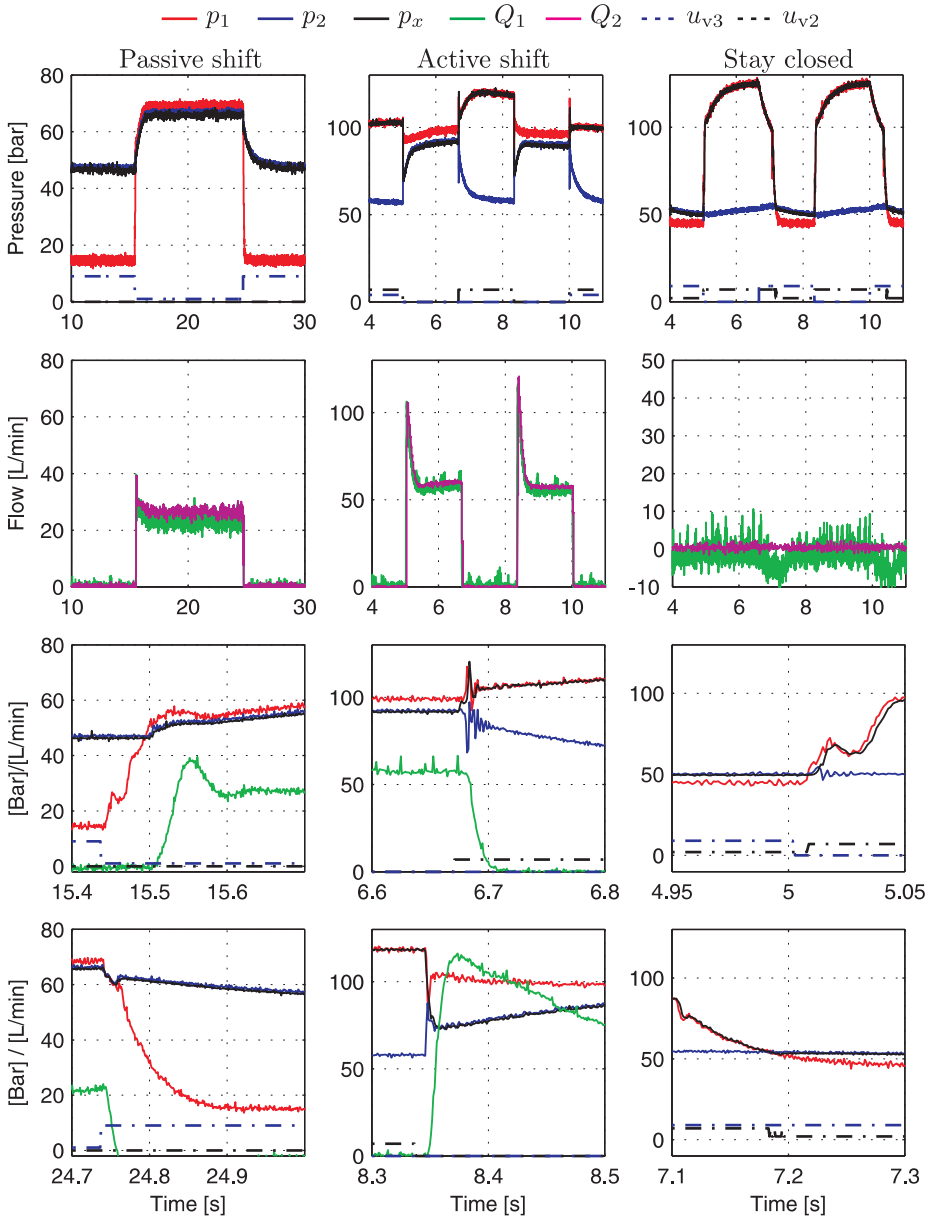

Figure 3.23: Measurements from the functionality test of the BC-valve concept. Results for Passive and active valve shifts are given along with results from the stay closed mode.

where $p_{\text{B.ref}} = [20\ 120\ 220]$ and the open and close signals are given at 0.15 s and 0.20 s respectively, see Fig. 3.24.

From the figure one must note that the closing of the valve is not depending on the system pressure level, contrary to the opening of the valve, which is seen to be highly dependent on the system pressure. However, both the opening and closing time is seen to be well under 10 ms, especially if excluding the delay from signal to valve movement. The delay is here partly due to delay of the pilot valve movement, but with the valve delay being consistent and well known (repeatable) a compensation strategy may be include in the

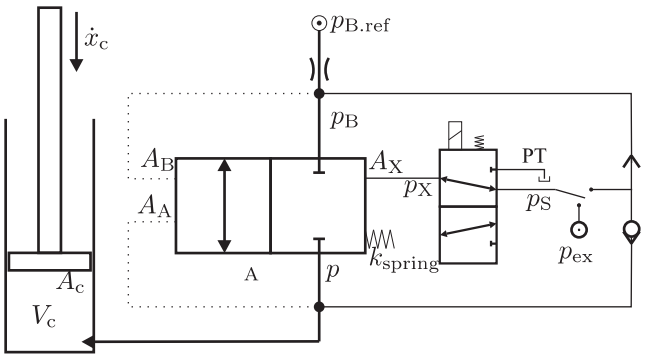

Figure 3.24: Valve test set-up, where the main stage from A to B is given as a multiple number of poppets. The pilot pressure is either taken from external p_{ex} or the internal shuttle valve.

n	Number of poppets	10
d	Inlet diameter	9.5mm
D	Poppet outer diameter	10mm
k_{spring}	Spring constant	1560N/m
$x_{pop.0}$	Initial spring compression	38mm
Δx_{pop}	Poppet stroke	2.5mm
	Pilot valve	FSVi 2.0*
	Pilot supply	Internal

Table 3.2: Valve parameter for on/off multi-poppet valve.

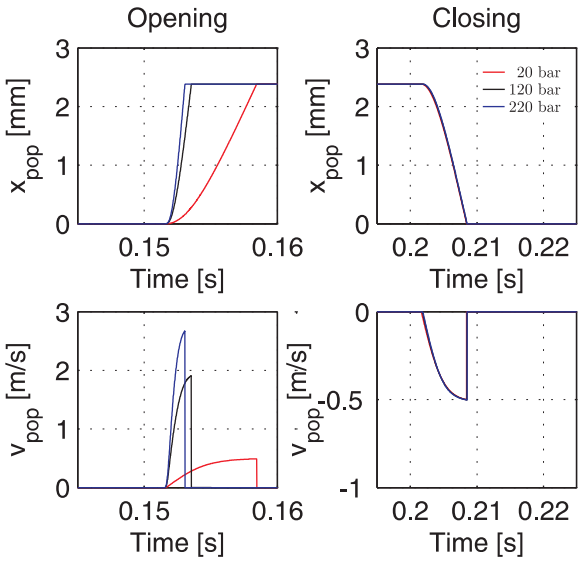

Figure 3.25: Poppet movement, with values from table 3.2 and system pressure of [20 120 220] bar.

force control to compensate for this.

3.4 Configuration of Switching Manifold

Based on the above findings for possible valve designs and the previous analysis of the feasibility of BCVs, it is found that the using BCVs in the switching manifold is feasible. However the optimal solution may also be a combination of utilising BCVs and on/off-valves in the switching manifold, where there is a potential in utilising the one directional check valves with stay opened and closed possibilities seen in Fig. 3.18 (d) and (e) in combination with the on/off valve in Fig. 3.18 (a). A concept for this type of novel manifold may be seen in Fig. 3.26. Here the one directional check valve with on/off possibilities is utilised for chamber connections to the low and high pressure line. Hereby the cylinder chambers will hydro-mechanically be connected to the low pressure if the chamber pressure drops below the low pressure line (without any control effort). Similarly the cylinder chambers will hydro-mechanically be connected to the high pressure line if the chamber pressure exceeds the high pressure line. The chambers connected to the medium pressure lines do however not require this functionality and they are hence simply fitted with on/off valves. This configuration of the manifold requires two types of pilot valves or pilot valve set-ups. The on/off valve for the mid pressure line requires a 3/2 pilot valve and a shuttle valve, whereas the one directional check valve with on/off possibilities on the other hand requires a 3/3 pilot valve and a shuttle valve. This may however be considered a feasible solution to include the above functionality.

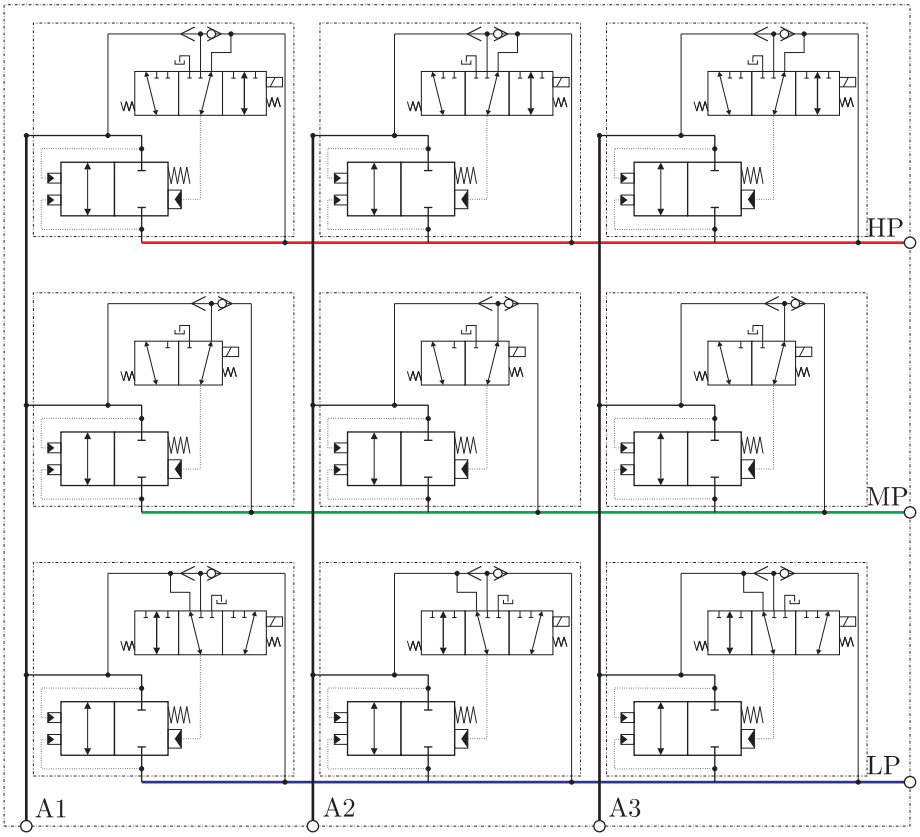

Figure 3.26: Schematic of a switching manifold utilising one directional check valve with on/off possibilities and on/off valves.

3.5 Summary

In this chapter different switching manifold configurations have been designed and investigated. Two different valve concepts have been considered and analysed and it has been shown that both bi-directional check valves (BCVs) and on/off-valves may be a feasible solution for the switching manifold, where the BCVs may partly reduce the need for accurate valve actuation, but at the possible expense of extra loading on the mechanical structure of the WECs. A prototype of an on-off valve based on the pilot stage from a Danfoss Power Solutions PVX-valve was developed and experimentally verified, indicating that this could meet the design specifications for the valve. The testing of the test bench however still remains. Similarly the concept for the bidirectional check valve was experimentally tested, hereby validating the feasibility of the concept.

Chapter 4

Test Bench and Experimental Findings

As basis for testing the PTO-system, a test bench has been designed at the university, see Fig. 4.1. The details of the design are presented in paper I. A figure of the test bench may bee seen in Fig. 4.1. The test bench was originally designed for testing a continuous PTO-system. A significant part of the work in the current project has therefore focused on installing the P1 prototype manifold on the test bench, see Fig. 4.2, developing new controllers for the wave side system, to accommodate the force spikes on the wave side system, due to the PTO force spikes, installation of sensors, etc. and commissioning the system, where the last commissioning is still ongoing. Yet the obtained test results are included in the following.

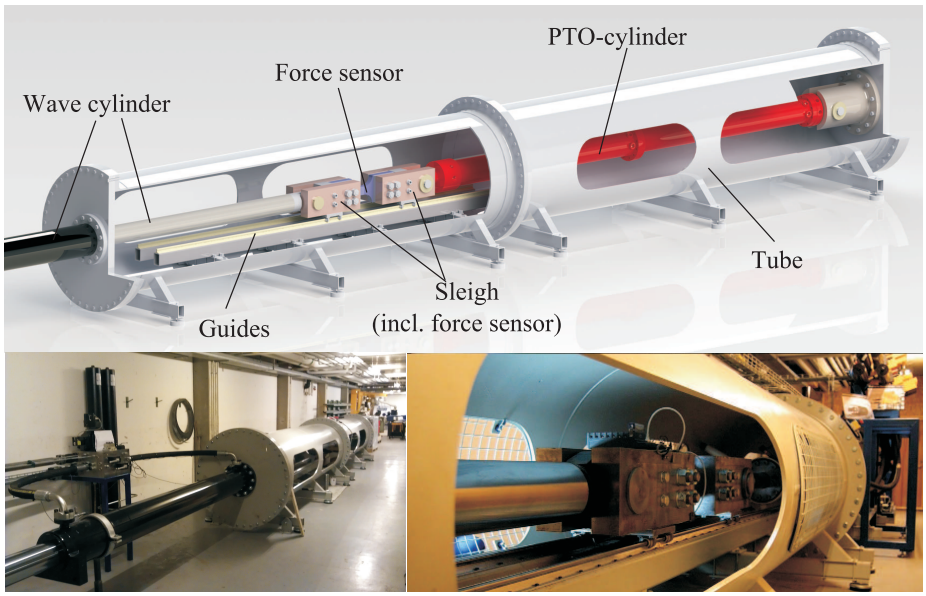

Figure 4.1: Illustration of the test-bench, [20].

The discrete fluid power PTO-system prototype tested consists of a five chamber multi-chamber cylinder and three common pressure lines, however the cylinder is operated as a three chamber cylinder by connecting some of the chambers in parallel. The valves employed in the switching manifold are fast 2/2 proportional valves. The proportionality and controllability of the switching valves enables a wide range of possibilities

in testing the influence of the valve opening characteristics on the system behaviour. Hence, the proportional valves are utilised for development purpose.

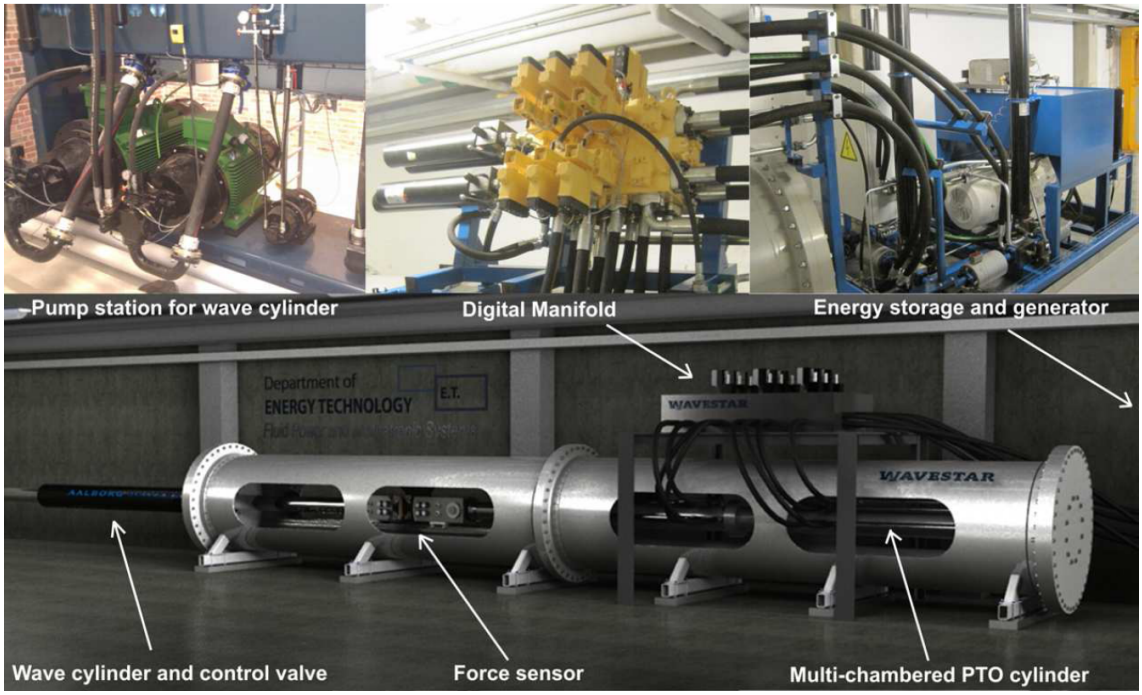

Figure 4.2: Illustration of the test bench and main components. In the upper row, the pump station (left), the P1 prototype (digital) manifold (centre) and the remaining PTO-system (energy storage and generator, right).

4.1 Modelling of the Test Bench

A simulation model is developed to facilitate controller design and testing of novel PTO control strategies. The modelling of the wave simulator is divided in three parts. First the mechanical motion, which is computed based on the pressure force delivered from the wave and the PTO cylinder respectively on the combined mechanical structure consisting of the wave piston, the PTO piston and the sleigh connecting the two pistons. Secondly, the fluid power system of the wave simulator cylinder is modelled and lastly the modelling of the PTO-system is described. For latter use the model is constructed such the PTO-system may easily be substituted with an other load system. A sketch of the fluid power system modelled is given in Fig. 4.3. The model derivation is given in [8], however two focus points are highlighted in the following. These are the servo valves for the wave simulator part as the control of these influence how well the system emulates the real system behaviour, and modelling of transmission lines for the PTO part as this also influence the pressure peaks and hence, if not included may influence the opening/pressure build up characteristics, resulting in deviations between the model and the physical system.

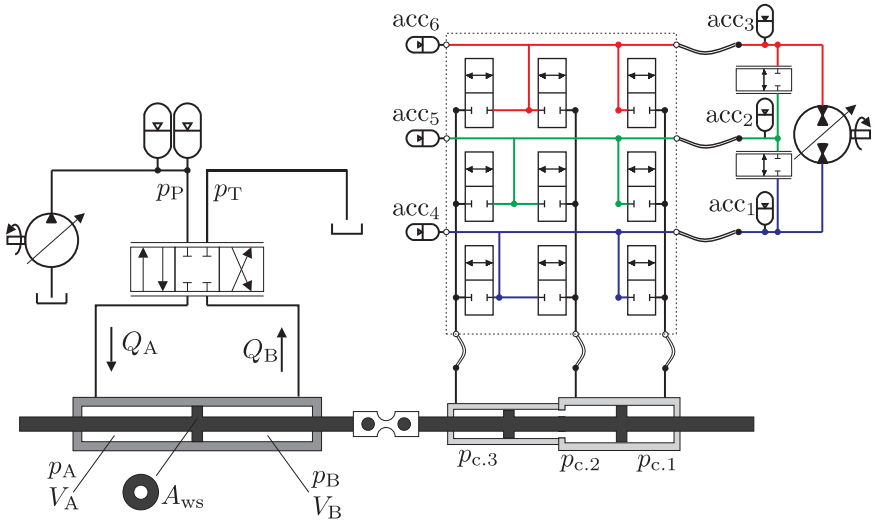

Figure 4.3: Sketch of the fluid power diagram, including the components included in the simulation model.

4.1.1 Servo Valves

Two servo valves are utilised in parallel, a large Parker D111FPE01 and a Moog D633 (100L/min). The opening area of the Parker valve is given in Fig. 4.4. It is seen that the Parker valve has an overlap spool with non-linear characteristic outside the lap area. Hence, some compensation of these non-linearities must be included in the control strategy. The Moog valve is here used to compensate for the dead band in the Parker valve, whereas implementation of this area characteristic in the simulation model is conducted by constructing a Lookup table in Simulink.

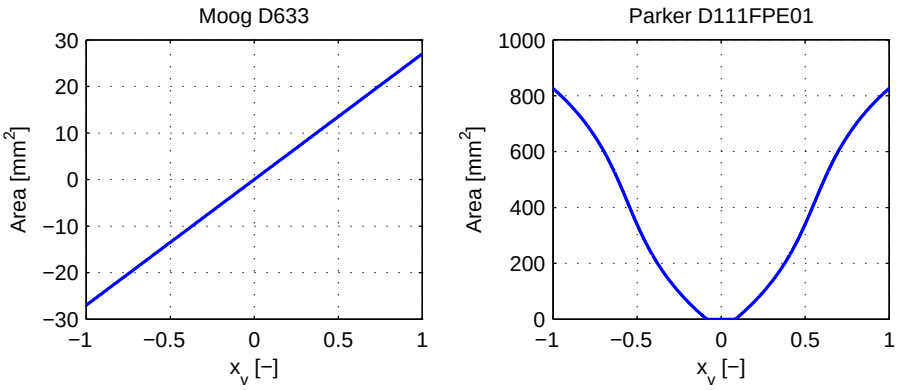

Figure 4.4: (a) Opening area for Moog valve as a function of nominal spool position. (b) Opening area for Parker valve as a function of nominal spool position.

The dynamics of the servo valves are modelled based on data sheet information. The dynamic of the Parker valve is modelled with a linear third order system in combination with a non-linear term to account for velocity saturation. The data sheet bode and the simulation model bode plot is seen in Fig. 4.5.

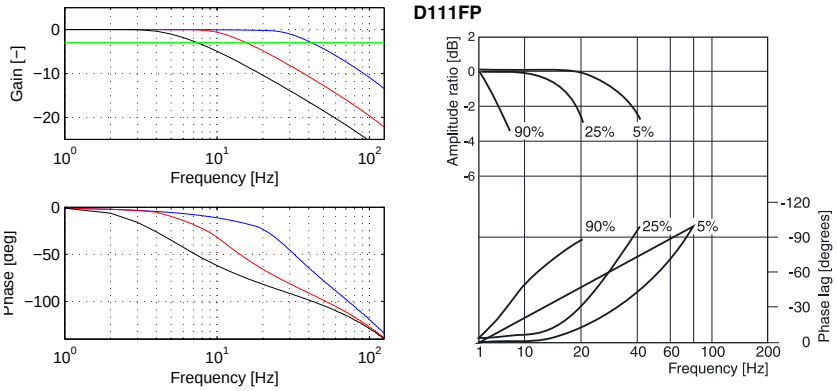

(a) (b)

Figure 4.5: (a) Opening area for Moog valve as a function of nominal spool position. (b) Opening area for Parker valve as a function of nominal spool position.

4.1.2 Transmission Lines

In the PTO-system transmission line models are imposed due to expected pressure oscillations in the hoses due to the fast opening and closing of the on/off valves connecting the cylinder chambers to the common pressure lines. The transmission line model utilised is a lumped parameter model where the transmission line is split into a fixed number of elements for which a pressure, a flow and a friction pressure is calculated, see Fig.4.6.

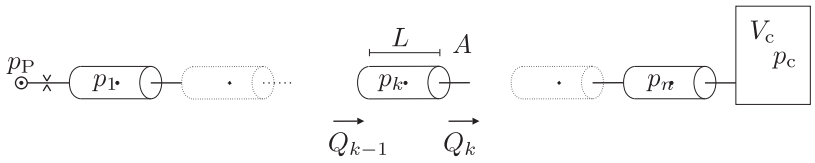

Figure 4.6: Illustration for the transmission line model.

Hence, the model include the acceleration of the inertia of the fluid in each element and the pressure build up in each element. Furthermore a friction modelled is included leading to a velocity dependant pressure loss. This model is illustrated in Fig. 4.7 for a hydraulic line with diameter 10 mm, where the blue line indicates the loss in a laminar regime whereas the red line is for the turbulent flow regime. The pressure loss used in the model is given by the black line.

4.2 Wave Emulation

The emulation of float movement is realised by feeding a reference wave and the physical PTO force to a float model. The output of this float model is then utilised as input reference to the wave simulator part of the test bench. This control structure is given in Fig. 4.8.

In the PhD dissertation [15] a state space controller for the wave cylinder is presented. Controller test results with this state space controller and various feedback additions are given in Fig. 4.9.

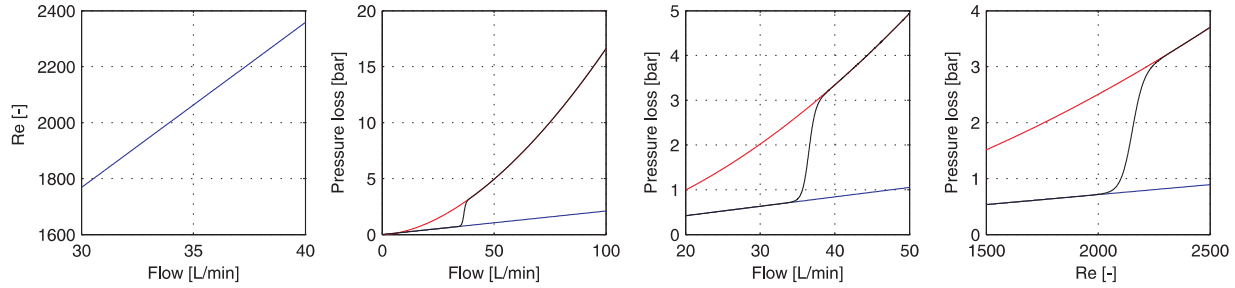

Figure 4.7: Friction model for transmission line. Upper left; Reynolds number based on flow. Upper right and lower left; Pressure loss based on flow. Lower right; Pressure loss based on Reynolds number.

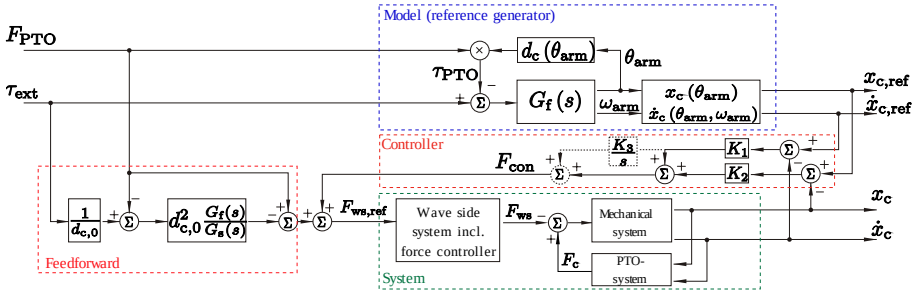

Figure 4.8: Control structure of the wave simulator.

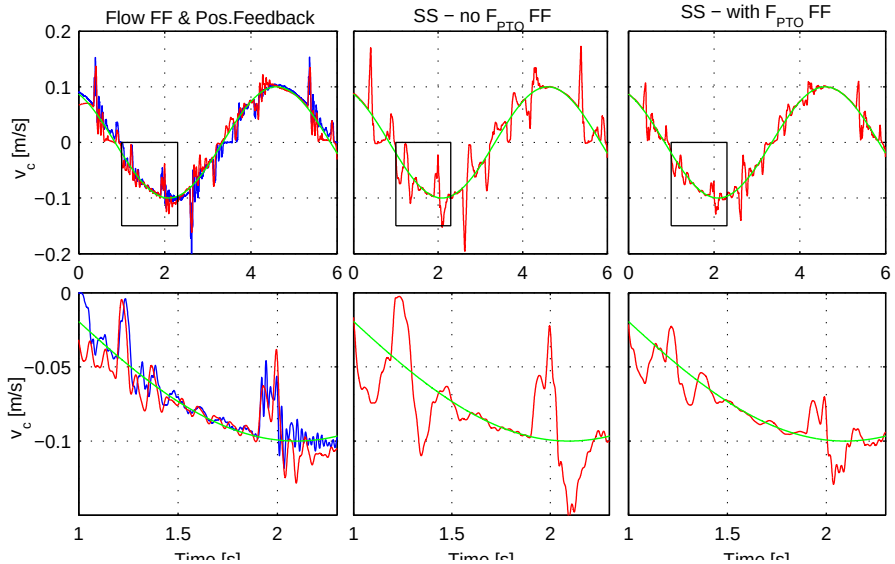

Figure 4.9: Controller tests. The blue curves are measured and red is simulated. The green is the velocity reference.

Here it is seen how the wave cylinder tracks a sinus reference while exposed to discrete loading due to force steps from the PTO system. The emulation of the float dynamics is tested in Fig. 4.10. Here clam water is assumed and the float is then pushed into and lifted out of the water and released respectively. It is seen

how the wave piston moves in a dampened oscillation as expected. It is furthermore seen, that for the case without PTO-force, there is exceptional correspondence between the simulated and measured response.

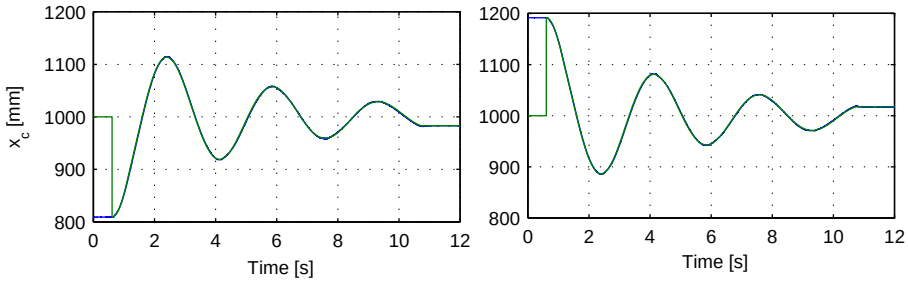

Figure 4.10: Control structure of the wave simulator.

4.2.1 Feedback Linearisation Controller

To reduce the influence from the force spikes on the wave side system, work has also gone into designed a controller based on the system model. With a good system model at hand a controller cancelling most non-linearities and external load may be designed. However, for thus a controller to work properly the model must be relative precise and state measurements are often required.

The controller type investigated is an input-output feedback linearisation controller, developed based on the system model on state space form:

$$\begin{aligned} \dot{\mathbf{x}}(t) &= \mathbf{f}(\mathbf{x}(t), u(t), t) \\ y(t) &= g(\mathbf{x}(t)) \end{aligned} \tag{4.1}$$

Where $\mathbf{x}(t)$ is the state vector, $u(t)$ is the input and $y(t)$ is the output. The system model is contained within the equations given in $\mathbf{f}(\mathbf{x}(t), u(t), t)$. Note that the system model is given as a single input single output model. For the given system the input is the spool reference for the servo valve and the output is either the piston position or velocity depending on the objective for the controller to be designed. As for most systems the output function $g(\cdot)$ does not explicitly contain the input $u(t)$ for the current system. Therefore the output $y(t)$ is differentiated as many times as required until the input $u(t)$ explicitly appears in the derivatives of $g(\cdot)$.

With the input directly contained in the function,

$$y^{(n)} = G(\mathbf{x}(t), u(t), t) \tag{4.2}$$

a input $u(t)$ is chosen such that:

$$y^{(n)} = v(t) \tag{4.3}$$

Hence, $u(t) = H(\mathbf{x}(t), v(t), t)$ with a new "controller" input v which as clearly seen directly controls the n'th derivative of the output y. The task in the controller design thereby becomes; to identify the linearisation term $H(\mathbf{x}(t), v(t), t)$ which cancels the system dynamics (linear and non-linear) and identify the new control input $v(t)$ which leads to a desired system behaviour. A schematic overview of the feedback linearisation controller developed is given in Fig. 4.11.

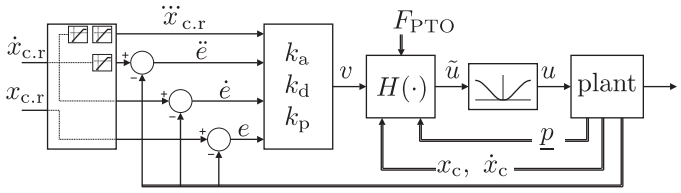

Figure 4.11: Illustration of the controller structure. The PTO force is seen as an external measured load.

4.2.2 Controller test

Simulation results with the designed feedback linearisation controller utilised are given in Fig. 4.12. A sinus wave is applied as position reference while imposing a discrete force step every 2.5 s. The controller is tested with the model assuming no PTO force and friction, and with the model assuming no PTO force, and lastly as shown in the controller design.

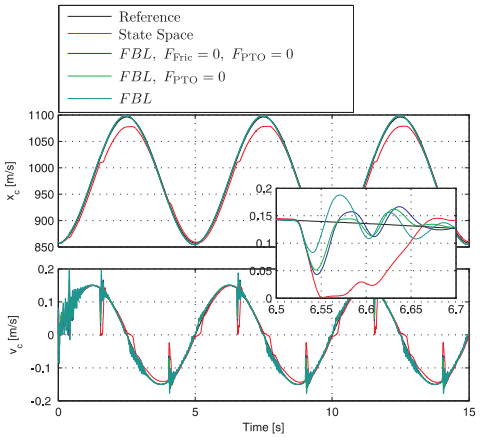

Figure 4.12: Piston velocity and position simulation results while utilising feedback linearisation controller.

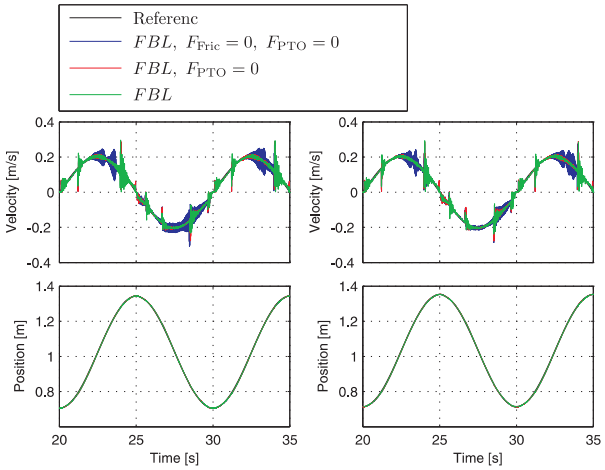

Figure 4.13: Piston velocity and position measurements while utilising feedback linearisation controller.

Measurements of piston velocity and position is seen in Fig. 4.13 for the test-bench when imposing the feedback linearisation controller. It is clearly seen that unwanted velocity oscillation are present even though the position measurements might look smooth. The velocity oscillations may partly be imposed due to controller input, this due to the fact that the control law utilises the acceleration as feedback. The acceleration feedback is currently performed by differentiation of the velocity measurements and hence suffers from problems with noise. Hence, to enable control by feedback linearisation an accelerometer is to be installed or other options as state estimation may be imposed. Before the validity and possible improvements of this results may be determined.

4.3 Test Results for Valve Shifts

Based on the controller described in section 4.2, it has however been possible to test the important characteristics of the system. These main results are presented in the following. In the following valve shifts are tested while the PTO cylinder piston is moved at a constant velocity, 0.3 m/s and -0.3 m/s respectively. The pressure characteristics in cylinder chamber 3 are given in Fig. 4.14 and 4.15 during pressure shifts with various valve switching times. The chamber pressure is shifted from high to low pressure and from low to high pressure in Fig.4.14 and 4.15 respectively. Here focus is on how the chamber pressure is changed prior to the new line connection is established. Hence, how much the pressure changes before the valve shift is accomplished.

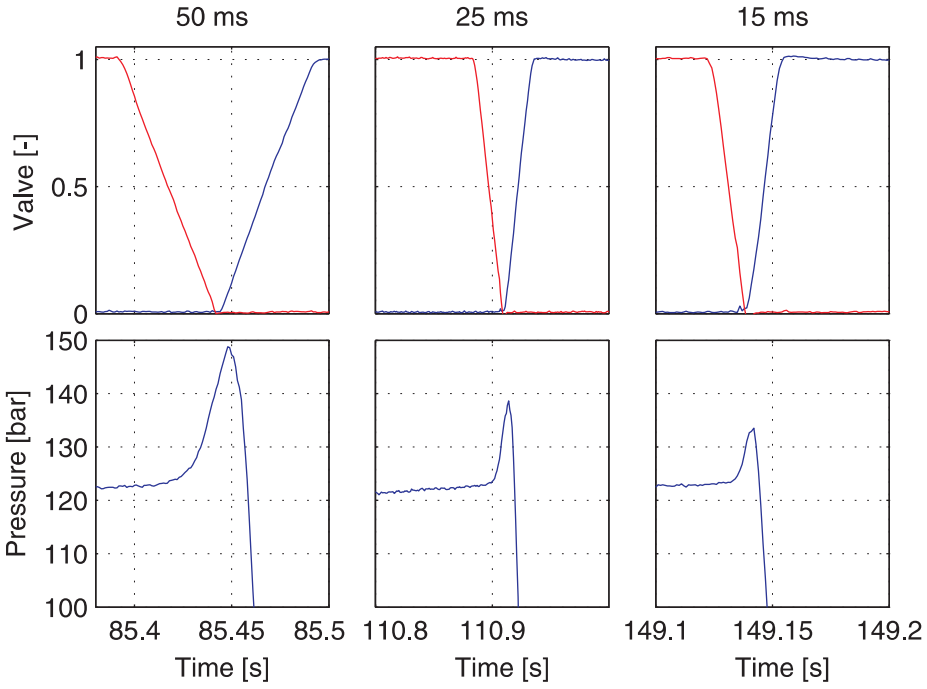

Figure 4.14: Pressure characteristics during high to low pressure shifts in PTO cylinder chamber 3 with constant piston velocity.

It is seen that a relative large switching time yield a large pressure increase or decrease respectively prior to the end of the valve shift. Hence, this supports the initial requirement on having valves with a switch time in the range of 15 ms seconds.

In Fig. 4.16 the chamber pressure characteristics just after a valve shift is seen, once again for varying valve switching time and piston velocities of 0.3 m/s and -0.3 m/s.

It is clearly seen in Fig. 4.16 that a faster valve switching yield large pressure oscillations in the cylinder chambers. Hence, with a low switching time only a small pressure peak is experienced before finishing the switching whereas large pressure oscillations are seen due to the fast valve switching.

Based on these findings, an improvement to the valve opening characteristics has been suggested, which may lower the pressure oscillations in the cylinder chamber due to a valve switching. The results hereof are presented in [15]. This improved valve switching characteristics and according pressure measurements are

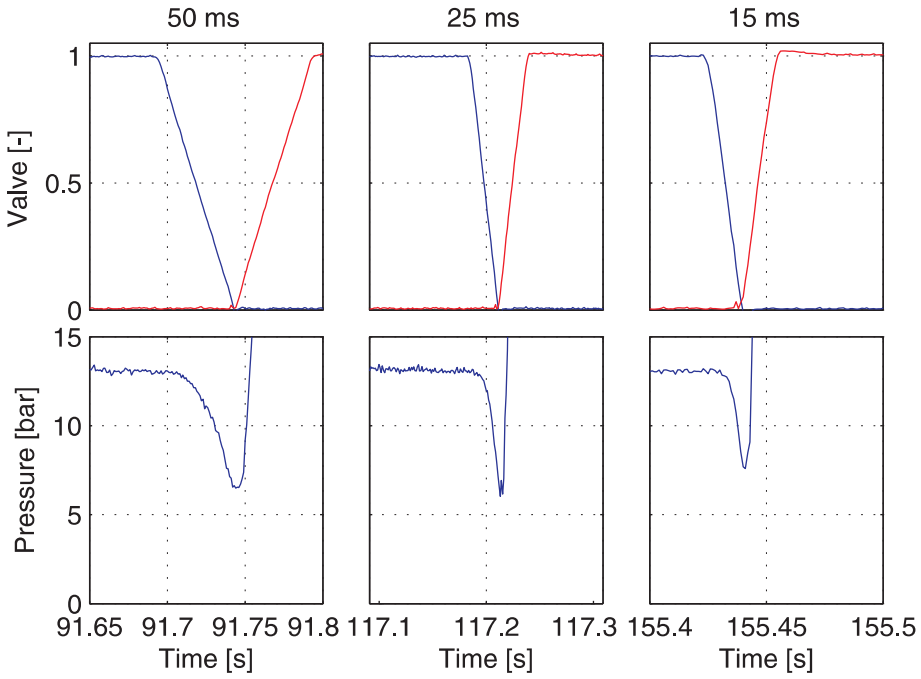

Figure 4.15: Pressure characteristics during low to high pressure shifts in PTO cylinder chamber 3 with constant piston velocity.

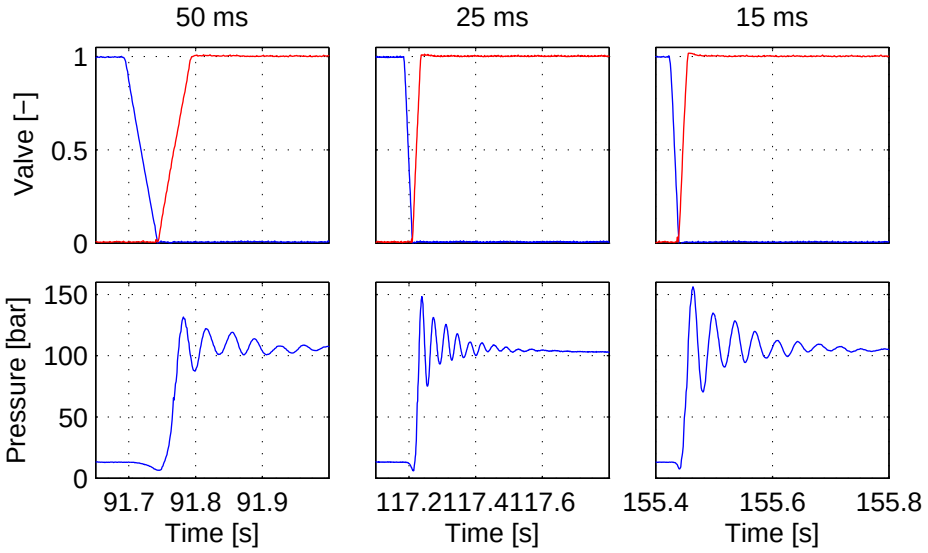

Figure 4.16: Pressure oscillation in PTO cylinder chamber 3 during pressure shifts for constant PTO cylinder speed.

seen in Fig. 4.17. Here it is compared with the nominal valve switching. For the improved valve switching valve closing is performed as in the normal valve switching, hence, a fast linear closing of the valves is performed. The valve opening is on the other hand performed in a small steep step and a long soft curve. As

clearly seen in Fig. 4.17 this improved valve shift significantly decreases the pressure oscillations, hence, this type of opening characteristic may therefore be sought after in the final valve design.

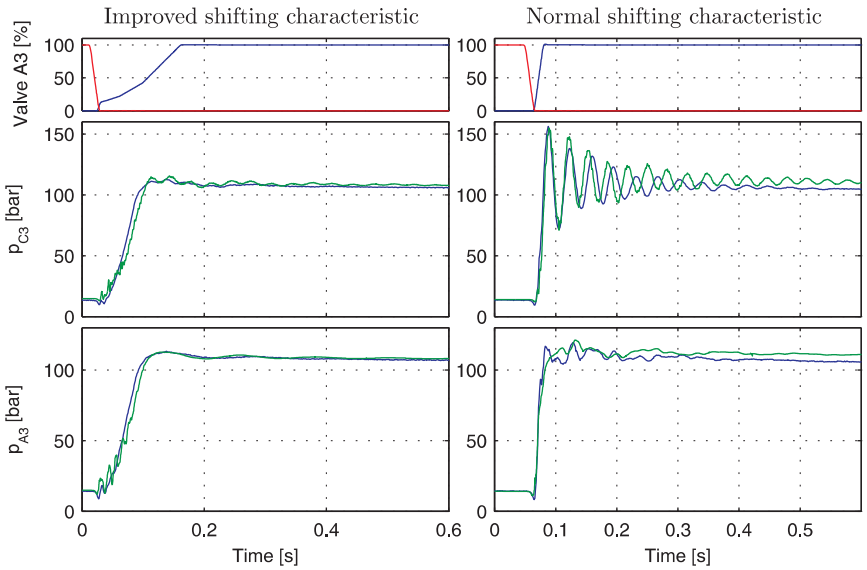

Figure 4.17: Test results with improved and normal shifts.

Note how the improved opening characteristic results in a very smooth pressure characteristic in the cylinder chamber. In addition the pressure at the switching manifold is seen to be very smooth, however the pressure change in the cylinder chamber is much slower for the improved valve opening. Hence, the avoidance of the pressure oscillations may be with a significant energy loss resulting.

However, based on these results future investigations should be focused on systems mimicking the improved shifts since the large pressure oscillations increase wear due to increased loading and cavitation in the cylinder chambers.

Despite not having conducted all tests then, based on the results obtained experimentally, it is possible to conclude that the models are in so good agreement with the physical system concerning pressures, flows, velocities etc., that the conclusions drawn from the simulation model are solid and that the expected and calculated efficiency of the system may be reached. It is furthermore found that the pressure spikes etc. are in so good agreement that the next iteration of the valve design should and will be based on the optimised opening characteristic, which the proportional has been used to emulate in the latest experiments.

Chapter 5

Conclusion

The focus of the current project has been on the analysis, development and design of a novel discrete force PTO concept for wave energy converters. The concept is based on a multi-chamber hydraulic cylinder, a number of common pressure lines from which power is extracted to the grid and a switching manifold, which is used to control, which of the pressure lines each of the cylinder chambers are connected to. The challenges in this regard relates to; determining the optimal number of pressure lines, the pressure level of these; the optimal number of chambers in the cylinder and the associated cylinder areas; developing/finding a suited valve technology and developing the switching manifold; and developing the control algorithm for how to control the valves. The conclusions of this work is outlined below.

The first chapter gave a short presentation of the problem at hand, outlined the major contributions of the work and discussed the deviations from the original project plan. Based on the proposed system a detailed study was made to determine how to optimally configure the WEC, the results of this was presented in chapter 2. From an initial analysis it was shown that even though an optimum could be found from simplified analysis, the problem at hand is complex, and the output of the system is highly dependent not only on the system configuration, but also the sea states, which the WEC is operating in. What is optimal for one sea state may therefore degrade performance for another. The optimal configuration of a discrete force system will therefore be highly dependent on wave conditions and wave spectrum in which the WEC is to be used. Similarly it was found that the energy output of the system is highly dependent on the systems configuration in terms of either the multi-chamber cylinder design or number of common pressure lines. Especially addition of extra pressure lines could result in an improvement in conversion efficiency. From the results given in section 2.6 a good energy production may hence be reached by utilising a two chamber symmetric cylinder and three pressure lines for which the pressure levels, however, should be controllable. Such a system configuration allows for utilisation of well proven cylinder technology with a simple construction. On the other hand the pressure line accumulators need to span a broader pressure range, resulting in an increasing accumulator capacity requirement. Going in the other direction and increasing the number of cylinder chambers, however also improves the system power extraction and reduces the need for extra pressure lines in the system. Common for the two solutions is, however that increasing the number of pressure lines or cylinders above three or four does not improve energy extraction significantly, and from a practical consideration the optimal solution may therefore be in the range of three pressure lines and three cylinder chambers, but with deviation here from dependent on the variation in sea states.

The energy extracted from the waves is in connection to the system configuration also highly dependent on the control algorithm for the system and two different force switching algorithms (FSAs) were presented, of

which the second showed slightly better results than the first in most cases. The strong coupling between the sea states and the optimal configuration of the system however means that in practice the sea conditions and wave spectrum dictates the optimal system configuration. A method for choosing a proper system configuration based on maximal energy output, taking into account the time distribution of sea conditions, was therefore developed and presented.

In the development of the switching manifold different valve concepts have been considered and investigated. The initial proposed switching manifold was based on using on/off-valves, an a valve solution was developed based on a Danfoss Power Solution PXE-pilot stage. Based on this, it was shown that it was possible to develop a valve with a switching time in the range of 15 ms, which could handle flow of up to 800 l/min with a pressure drop below 1.5 bar in both directions. The valve was partly experimentally validated, showing good agreement between modelled and measured behaviour, and based on these findings it was found that the valve fulfilled the design requirements, when to be used in the switching manifold. The full testing of the valve in the switching manifold however still remains, as the full scale test set-up has been delayed.

Secondly an alternative valve concept, in form of a bidirectional check valve (BCV) has been investigated and compared with the on/off valve solution. The benefit of the BCV is that it partly reduces the need for accurate valve actuation as this is handled hydro-mechanically, based on the pressure in the cylinder chambers. A feasibility study of this valve concept was presented, describing how the pressure dynamics in the cylinder chambers may help to open/close the valves and two valve concepts for respectively an on/off valve and a BCV multi-poppet valve was developed and compared in simulation. The results from the simulation showed that the BCV was a feasible concept and that it could reduce the number of timed actuations of the valves, but that this was at the possible expense of extra loading on the mechanical structure of the WEC. The BCV concept was furthermore experimentally validated, showing that the functionality of the concept could be obtained and with acceptable switching times. Based on the analysis a proposal for a new switching manifold utilising both BCVs and on/off-valves was furthermore developed, the benefit of which is that this incorporates extra safety, whereby the cylinder pressures do not exceed the pressure in the high pressure line and similarly that the cylinder pressure do not drop below the pressure in the low pressure line.

Finally results obtained with the first prototype switching manifold in the full test bench was presented, which validated the feasibility of the switching manifold/discrete force concept. This included a discussion of the control algorithms developed for the test bench, their implementation and results which validates the developed models of the test set-up. Due to a delayed commissioning of the test bench, only part of the planned experimental results have been obtained. However, the simulated model behaviour is in so good agreement with the experimental results that the results obtained from the simulation models are considered with a high level of confidence. From the experimental results obtained, it was validated that the valve switching time directly affects the cylinder pressures and that pressure oscillations are experienced in the transmission lines from manifold to the cylinder chambers. Based on these results a modified shifting characteristic was also developed and tested (emulated) on the test set-up, whereby the pressure oscillations in the transmission lines were effectively removed. Further work will therefore focus on these modifications and a full validation of the switching manifold.

Bibliography

[1] A. H. Hansen, R. H. Hansen, and H. C. Pedersen. Optimal number of pressure lines in a discrete hydraulic force system for the pto-system in wave energy converters. In *Proc. of the 7th FPNI PhD symposium on Fluid Power.*, 2012.

[2] A. H. Hansen, R. H. Hansen, and H. C. Pedersen. Optimisation of working areas in discrete hydraulic power take off-system for wave energy converters. In *Proc. of the fifth Workshop on Digital Fluid Power.*, 2012.

[3] A. H. Hansen and H. C. Pedersen. Optimal configuration of discrete fluid power system utilised in the pto for wecs. *Submitted for publication in Ocean Engineering - An International Journal of Research and Development*, -:–, -.

[4] A.H. Hansen, H.C. Pedersen, and T.O. Andersen. Design of a multi-poppet on-off valve for wave energy converters. In *Proc. of 2013 IEEE International Conference on Mechatronics and Automation.*, 2013.

[5] A.H. Hansen, H.C. Pedersen, and T.O. Andersen. Design of bidirectional check valve for discrete fluid power force system for wave energy converters. In *Proc. of ASME/Bath Symposium on Fluid Power & Motion Control, FPMC2013.*, 2013.

[6] A.H. Hansen, H.C. Pedersen, and T.O. Andersen. On/off multi-poppet valve for switching manifold in discrete fluid power force system pto in wave energy converters. *Accepted for publication in; International Journal of Mechatronics and Automation.*, -:–, 2014.

[7] Anders H. Hansen and Henrik C. Pedersen. Optimal discrete pto force for point absorber wave energy converters in regular waves. In *10th European Wave and Tidal Energy Conference 2013*, 2013.

[8] Anders Hedegaard Hansen. *Investigation and Optimisation of a Discrete Fluid Power PTO-system for Wave Energy Converters*. PhD thesis, Faculty of Engineering and Science at Aalborg University, 2014.

[9] Anders Hedegaard Hansen, Henrik C. Pedersen, and Torben O. Andersen. Model based feasibility study on bidirectional check valves in wecs. *Submitted to Int. Journal of Marine Energy*, 2014.

[10] R.H. Hansen, T.O. Andersen, and H.C. Pedersen. Determining required valve performance for discrete control of pto cylinders for wave energy. In Nigel Johnston and Andrew R. Plummer, editors, *Proc. of Bath/ASME Symposium on Fluid Power and Motion Control, FPMC 2012*. American Society of Mechanical Engineers, 2012.

[11] R.H. Hansen, A.H. Hansen, and T.O. Andersen. Influence and utilisation of pressure propagation in pipelines for secondary controlled discrete displacement cylinders. *Applied Mechanics and Materials*, 233:72–75, 2012.

[12] R.H. Hansen, A.H. Hansen, and T.O. Andersen. Simulation of utilisation of pressure propagation for increased efficiency of secondary controlled discrete displacement cylinders. *Applied Mechanics and Materials*, 233:3–6, 2012.

[13] Rico H. Hansen, Torben O. Andersen, and Henrik C. Pedersen. Analysis of discrete pressure level systems for wave energy converters. In *International Conference On Fluid Power And Mechatronics*, 2011.

[14] Rico H. Hansen and Morten M. Kramer. Modelling and control of the wavestar prototype. In *EWTEC 2011*, 2011.

[15] Rico Hjern Hansen. *Design and Control of the Power Take-Off System for a Wave Energy Converter with Multiple Absorbers.* PhD thesis, Faculty of Engineering and Science at Aalborg University, 2013.

[16] Morten Kramer, Laurent Marquis, and Peter. Frigaard. Performance evaluation of the wavestar prototype. In *Proceedings of the 9th European Wave and Tidal Conference, 9th ewtec 2011*, 2011.

[17] M. Linjama, H-P. Vihtanen, A. Sipola, and M. Vilenius. Secondary controlled multi-chamber hydraulic cylinder. In *The 11th Scandinavian International Conference on Fluid Power, SICFP09, June 2-4, 2009, Linköping, Sweden*, 2009. WE3.1.3.1, ME1.1.1.

[18] Herbert E. Merritt. *Hydraulic Control System*. John Wiley & Sons, Inc., 1967.

[19] Inc Ocean Power Technologies. www.oceanpowertechnologies.com. Viewed 03/2011.

[20] H.C. Pedersen, A.H. Hansen, R.H. Hansen, T.O. Andersen, and M.M. Bech. Design and control of full scale wave energy simulator system. In *Proc. Bath/ASME Symposium on Fluid power and Motion Control, FPMC2012.*, 2012.

[21] Pelamis Wave Power. *Pelamis P-750 Wave Energy Converter*. Pelamis Wave Power.

[22] M.H. Sørensen, M.H. Sørensen, and M. Højen. Design of a fast switching hydraulic valve. Master's thesis, Aalborg University, The Energy Study Board, Mechatronic Control Engineering Supervisors: H.C. Pedersen & Anders H. Hansen, 2012.

[23] WaveStarA/S. www.wavestarenergy.com.